the plant journal

S E B
SOCIETY FOR EXPERIMENTAL BIOLOGY

ERFVII-controlled hypoxia responses are in part facilitated by MEDIATOR SUBUNIT 25 in *Arabidopsis thaliana*

Jos H. M. Schippers[1,*], Kira von Bongartz[2,†], Lisa Laritzki[2,†], Stephanie Frohn[1,†], Stephanie Frings[3,4,†],
Tilo Renziehausen[3,4,†], Frauke Augstein[5], Katharina Winkels[2], Katrien Sprangers[6], Rashmi Sasidharan[7],
Didier Vertommen[8], Frank Van Breusegem[9,10], Sjon Hartman[11,12], Gerrit T. S. Beemster[6], Amna Mhamdi[9,10],
Joost T. van Dongen[2] and Romy R. Schmidt-Schippers[3,4,*]

[1]Department of Molecular Genetics, Seed Development, Leibniz Institute of Plant Genetics and Crop Plant Research (IPK),
Corrensstraße 3, Gatersleben, Seeland 06466, Germany,

[2]Institute of Biology I, RWTH Aachen University, Worringerweg 1, Aachen 52074, Germany,

[3]Plant Biotechnology, Faculty of Biology, University of Bielefeld, Universitätsstraße 25, Bielefeld 33615, Germany,

[4]Center for Biotechnology, University of Bielefeld, Universitätsstraße 27, Bielefeld 33615, Germany,

[5]Department of Organismal Biology, Physiological Botany, and Linnean Centre for Plant Biology, Uppsala University, Ullsv.
24E, Uppsala SE-75651, Sweden,

[6]IMPRES Research Group, Department of Biology, University of Antwerp, Groenenborgerlaan 171, G.U.613, Antwerpen 2020,
Belgium,

[7]Plant Stress Resilience, Institute of Environmental Biology, Utrecht University, Padualaan 8, Utrecht 3584 CH, The Netherlands,

[8]de Duve Institute and MASSPROT platform, Université Catholique de Louvain, Avenue Hippocrate 75, Brussels 1200, Belgium,

[9]Department of Plant Biotechnology and Bioinformatics, Ghent University, Technologiepark 71, Ghent 9052, Belgium,

[10]Vlaams Instituut voor Biotechnologie (VIB), Center for Plant Systems Biology, Technologiepark 71, Ghent 9052, Belgium,

[11]CIBSS – Centre for Integrative Biological Signalling Studies, University of Freiburg, Schänzlestraße 18, Freiburg 79104, Germany, and

[12]Plant Environmental Signalling and Development, Faculty of Biology, University of Freiburg, Schänzlestraße 1, Freiburg
79104, Germany

SUMMARY

Flooding impairs plant growth through oxygen deprivation, which activates plant survival and acclimation responses. Transcriptional responses to low oxygen are generally associated with the activation of group VII ETHYLENE-RESPONSE FACTOR (ERFVII) transcription factors. However, the exact mechanisms and molecular components by which ERFVII factors initiate gene expression are not fully elucidated. Here, we show that the ERFVII factors RELATED TO APETALA 2.2 (RAP2.2) and RAP2.12 cooperate with the Mediator complex subunit *At*MED25 to coordinate gene expression under hypoxia in *Arabidopsis thaliana*. Respective *med25* knock-out mutants display reduced low-oxygen stress tolerance. *At*MED25 physically associates with a distinct set of hypoxia core genes and its loss partially impairs transcription under hypoxia due to decreased RNA polymerase II recruitment. Association of *At*MED25 with target genes requires the presence of ERFVII transcription factors. Next to ERFVII protein stabilisation, also the composition of the Mediator complex including *At*MED25 is potentially affected by hypoxia stress as shown by protein-complex pulldown assays. The dynamic response of the Mediator complex to hypoxia is furthermore supported by the fact that two subunits, *At*MED8 and *At*MED16, are not involved in the establishment of hypoxia tolerance, whilst both act in coordination with *At*MED25 under other environmental conditions. We furthermore show that *At*MED25 function under hypoxia is independent of ethylene signalling. Finally, functional conservation at the molecular level was found for the MED25-ERFVII module between *A. thaliana* and the monocot species *Oryza sativa*, pointing to a potentially universal role of MED25 in coordinating ERFVII-dependent transcript responses to hypoxia in plants.

Keywords: hypoxia, flooding, Mediator complex, transcription, ERFVII factors.

INTRODUCTION

Increased frequencies of heavy rainfall due to climate change have made flooding one of the most prevalent and severe abiotic stresses threatening agricultural production (Liu et al., 2023). Flooding stress can occur in the form of submergence of the whole plant or waterlogging, which primarily affects the root system. Either way, flooding represents a major detrimental event leading in the long-term to plant death. Since flooding impairs oxygen diffusion, aerobic respiration for providing energy equivalents is hampered or even blocked. To adapt, plants will induce an acclimation response, including activation of anaerobic respiration, a process that is under strict transcriptional control (Bailey-Serres et al., 2012; Renziehausen et al., 2024).

Acclimation to hypoxia in plants is mediated by a multitude of transcription factors (Eysholdt-Derzsó et al., 2023; Gasch et al., 2016; Tang et al., 2021), but group VII ETHYLENE-RESPONSE FACTOR (ERFVII) transcription factors play a key role in transcriptional reprogramming and subsequent metabolic switching in Arabidopsis and crops (Giuntoli & Perata, 2018; Loreti & Perata, 2023). The most prominent ERFVII member is SUBMERGENCE 1A (SUB1A) which has been successfully used to breed submergence-tolerant rice varieties (Bailey-Serres et al., 2010). Genes regulated by SUB1A participate in various processes, including growth, scavenging of reactive oxygen species and anaerobic metabolism (Fukao et al., 2011; Locke et al., 2018; Xu et al., 2006). Moreover, SUB1A directly transcriptionally activates two other ERFVII members, ERF66 and ERF67 during submergence, which in turn activates fermentative pathway genes (Lin et al., 2019). In Arabidopsis, the ERFVII family contains five members, which all have been implicated in flooding tolerance, including RELATED TO APETALA 2.2 (RAP2.2; Hinz et al., 2010), RAP2.3 (Papdi et al., 2015), RAP2.12 (Licausi et al., 2011) and HYPOXIA RESPONSIVE ERF 1 (HRE1) and HRE2 (Licausi et al., 2010). ERFVII-controlled genes in both rice and Arabidopsis comprise fermentative genes, such as PYRUVATE DECARBOXYLASE 1 (PDC1) and ALCOHOL DEHYDROGENASE 1 (ADH1) compensating for impaired ATP synthesis under limited oxygen availability (Licausi et al., 2011; Locke et al., 2018). Arabidopsis ERFVII proteins are controlled in their stability by the current intracellular oxygen concentration, as they are substrates of the PLANT CYSTEINE OXIDASE (PCO)-dependent branch of the PROTEOLYSIS 6 (PRT6) N-degron pathway (Licausi et al., 2011; White et al., 2017, 2018). Whilst in rice, ERF66 and ERF67 are N-degron substrates (Lin et al., 2019), SUB1A is not degraded by this pathway (Gibbs et al., 2011). Constitutively expressed RAP-type ERFVII factors can be stored in the plasma membrane where they are protected from proteolysis. For instance, in Arabidopsis, RAP2.12 resides

under aerobic conditions at the plasma membrane through interaction with ACYL-COA BINDING PROTEIN 1 (ACBP1) but translocates to the nucleus during low-oxygen conditions upon an energy-related lipid signal (Licausi et al., 2011; Schmidt et al., 2018; Zhou et al., 2020). Whilst the regulation of hypoxia core genes (HCGs) by ERFVII factors is well documented (e.g. Bui et al., 2015; Gibbs et al., 2011; Licausi et al., 2011), direct binding of these transcription factors to specific cis-elements in target promoters has been less studied. RAP2.2, RAP2.12 and to a lesser extent RAP2.3 act redundantly as principle activators of hypoxia-responsive genes by recognising the HYPOXIA-RESPONSIVE PROMOTER ELEMENT (HRPE) within hypoxia-responsive target promoters (Gasch et al., 2016). Interestingly, on the other hand, HRE2 binds to promoter regions containing a GCC-rich EBP-like box (Lee & Bailey-Serres, 2019), which is commonly present in promoters that also contain an HRPE, suggesting that HCGs are transcriptionally activated by one or more ERFVII factors. In addition, RAP2.3 promotes apical hook formation and is linked to the ethylene signalling pathway, whereby ethylene promotes nuclear RAP2.3 localisation (Kim et al., 2018). Finally, ERFVII protein abundance and action are controlled by additional environmental cues that include nitric oxide (NO) depletion and retrograde signals (Barreto et al., 2022; Gibbs et al., 2014; Hartman et al., 2019). Although it is relatively well known which transcriptional targets ERFVII factors have and how their protein turnover is controlled, it is not yet clear how they initiate transcription of their target genes. Especially components that enable ERFVII proteins to relay hypoxia stress signals to the cellular transcriptional machinery and which themselves are part of a regulatory mechanism under stress, that is, beyond ERFVII stabilisation, are so far elusive.

To activate transcription, transcription factors must recruit the cellular transcriptional machinery consisting of RNA polymerase II (RNAPII) and general transcription factors to target promoters. Importantly, the integration of stress signals and linkage of stress-related transcription factors with RNAPII requires specific coactivators. Originally identified in yeast, the highly dynamic multi-subunit Mediator complex is able to facilitate stress-specific transcription across all eukaryotes (Kornberg, 2005). In Arabidopsis, the Mediator core complex consists of 32 subunits forming three distinct modules: Head, Middle and Tail (Mathur et al., 2011). In addition, the Kinase module composed of CYCLIN-DEPENDENT KINASE 8 (CDK8), AtMED12, AtMED13 and CDK8-associated cyclin (CycC) (Mathur et al., 2011) is associated with the core complex, of which CDK8 itself has been reported to possess repressor activity but also to positively affect transcription initiation (Gonzalez et al., 2007; Zhu et al., 2014). Whilst the Head module

contacts with RNAPII, the Tail module determines gene-specific functions by interacting with *cis*-acting transcription factors (Dotson et al., 2000). Importantly, instead of being a passive component of the cellular transcriptional machinery, its plasticity in incorporating different subunits allows the Mediator complex to integrate a wide variety of environmental signals. Tailored stress responses mediated by the Mediator complex not only rely on its interaction with specific transcription factors but also the complex itself is modulated under stress, for example, through direct post-translational modifications of individual Mediator subunits, resulting in changing subunit abundance, localisation and/or activity (Henke et al., 2011; Miller et al., 2012).

In Arabidopsis and rice, individual Mediator subunits have been shown to modulate transcript responses tailored to specific environmental cues, including pathogen stress (Li et al., 2018; Suzuki et al., 2022; Zhang et al., 2023), hormone signalling (Agrawal et al., 2022; An et al., 2017; Guo et al., 2022; Ito et al., 2016; Wang et al., 2019), secondary metabolism (Dolan et al., 2017), root growth (Zhang et al., 2018), fatty acid biosynthesis (Kim et al., 2016) and iron uptake (Zhang et al., 2014). The Arabidopsis Mediator subunit 25 (*At*MED25) was initially identified as a regulator of developmental processes, for example, flowering time (Bäckström et al., 2007; Cerdan & Chory, 2003), lateral root growth and root hair differentiation (Raya-Gonzalez et al., 2014; Sundaravelpandian et al., 2013). *At*MED25 modulates jasmonic acid, abscisic acid and ethylene signalling and is therefore key to plant stress responses and signalling pathways (An et al., 2017; Chen et al., 2012; Yang et al., 2014). Regarding stress conditions, *At*MED25-mediated transcription contributes to tolerance towards salinity and pathogen attack, whilst a negative role for *At*MED25 was shown for drought stress (Çevik et al., 2012; Elfving et al., 2011; Kidd et al., 2009; Ou et al., 2011; Zhu et al., 2014). To execute its function, *At*MED25 physically interacts with diverse stress-related transcription factors, for example, DEHYDRATION RESPONSIVE ELEMENT-BINDING PROTEIN (DREB2A), ABA INSENSITIVE5 (ABI5) and several AP2/ERF transcription factors (Çevik et al., 2012; Chen et al., 2012; Elfving et al., 2011; Ou et al., 2011), which represent important regulators of transcriptional responses to drought and temperature stress. Intriguingly, *At*MED25 also interacts with the hypoxia-related ERFVII factor RAP2.2 (Ou et al., 2011), suggesting a potential role for *At*MED25 in regulating responses specific to hypoxia.

In the present study, we report that *At*MED25 interacts with the hypoxia-related ERFVII factors RAP2.2 and RAP2.12 from Arabidopsis and contributes to their ability to activate the transcription of hypoxia-responsive genes. In addition, consistent with ERFVII factor stabilisation under low-oxygen stress, *At*MED25 associates with ERFVII-controlled promoters specifically under hypoxia for optimal recruitment of RNAPII to modulate gene expression. Concomitantly, expression of hypoxia-responsive genes in stressed *med25* knock-out mutants is impaired but not fully abolished, suggesting that ERFVII factors, as also shown for hypoxia-specific transcription factors in humans, act in concert with multiple transcriptional activators. Of note, *At*MED25 and the Mediator complex composition itself appear to be affected by hypoxia as shown by affinity purification assays. Proteins interacting with *At*MED25 in part seem to differ under normoxia and hypoxia. Notably, the subunit's cooperation with two other Mediator core subunits, otherwise required for regulating flowering time and iron deficiency responses, respectively, is not needed under hypoxia stress. These findings in combination support a dynamic response of the Mediator complex to low-oxygen conditions. Furthermore, we show that the MED25-ERFVII module is also present in the monocot model plant *Oryza sativa*. Taken together, our work supports an interplay between ERFVII factors and the Mediator complex involving MED25 to enable fine-tuning of transcriptional responses to hypoxia.

RESULTS

ERFVII factors interact with the mediator complex subunit *At*MED25

The Arabidopsis ERFVII factor RAP2.2 was previously identified in a high-throughput screening system for transcription factors interacting with *At*MED25 (Ou et al., 2011). To validate the interaction between RAP2.2 and *At*MED25, and to determine if other ERFVII members can interact with *At*MED25 as well, targeted protein–protein interaction assays were performed. First, protein–protein interaction studies in yeast using full-length *At*MED25 in combination with all five Arabidopsis ERFVII transcription factors, namely RAP2.2, RAP2.12, RAP2.3, HRE1 and HRE2 were conducted (Figure 1A). *At*MED25 interacted with both RAP2.2 and its homologue RAP2.12. Subsequently, *At*MED25-RAP2.2 and *At*MED25-RAP2.12 binding was validated in an *in vitro* pulldown approach using CFP-tagged ERFVII proteins and FLAG-tagged *At*MED25 protein (Figure 1B). *In planta*, *At*MED25-GFP fusion protein exhibited nuclear localisation under both normoxic and hypoxic conditions (Figure 1C). Accordingly, in a follow-up bimolecular fluorescence complementation (BiFC) assay with *At*MED25 and the two ERFVII factors, protein complexes were solely detectable in the nucleus (Figure 1D). Next, we examined the capability of other Mediator subunits besides *At*MED25 to interact with RAP2.2 and RAP2.12. Eight Mediator subunits, namely *At*MED8, *At*MED16, *At*MED19, *At*MED21, *At*MED28, *At*MED32, *At*MED34 and *At*MED36 were selected based on their localisation in the Tail or Middle module of the Mediator complex. The Tail module
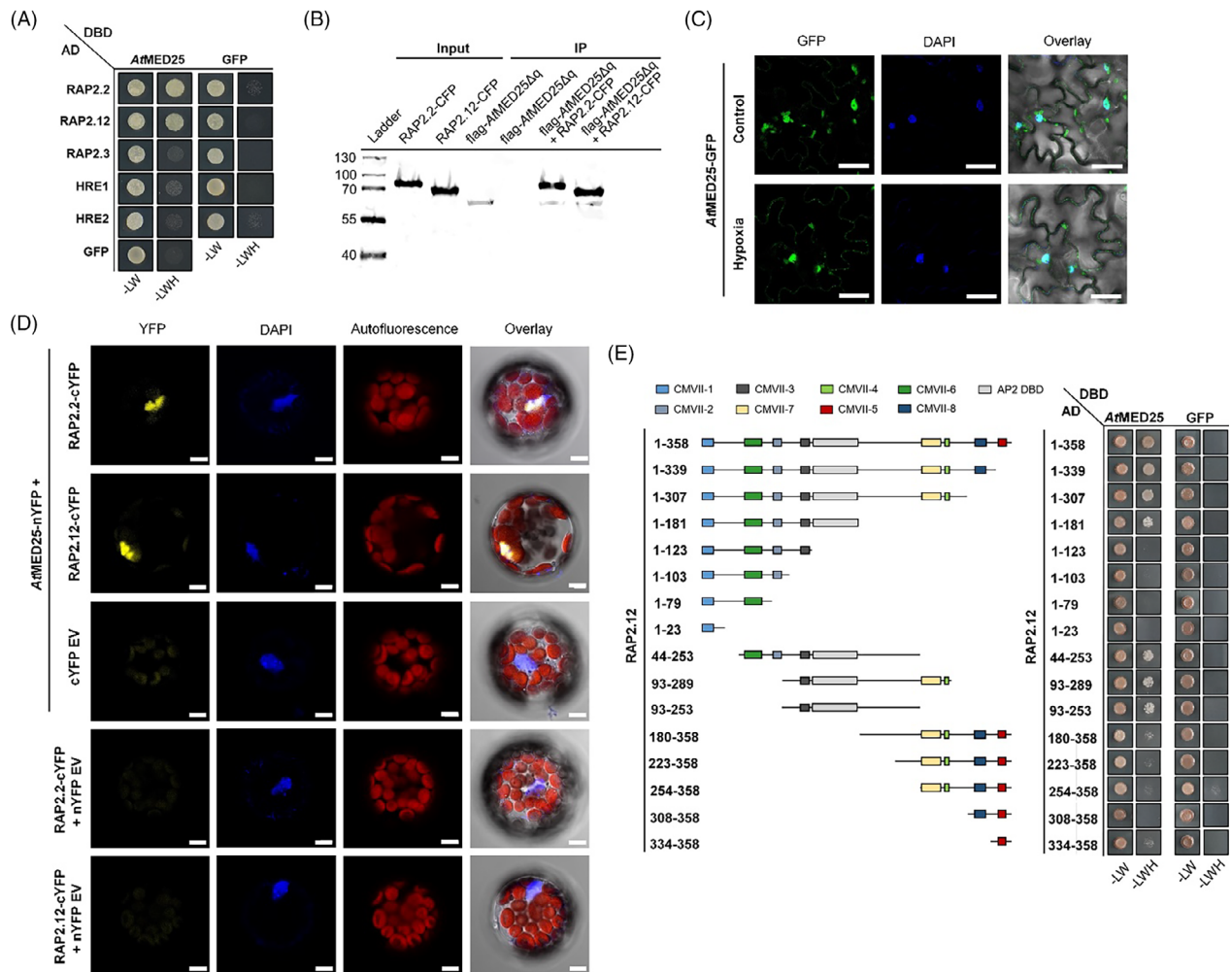
Figure 1. Physical interaction between Mediator subunit *At*MED25 and ERFVII factors.

(A) Yeast two-hybrid analysis of the interaction between *At*MED25 and five ERFVII factors from Arabidopsis. *At*MED25 fusion with the GAL4 DNA binding domain (DBD) was co-transformed into yeast with ERFVII factors fused to the GAL4 activation domain (AD) and selected on synthetic dropout (SD) medium lacking leucine and tryptophan (−LW). Protein interactions were tested on an SD medium lacking leucine, tryptophan and histidine (−LWH) in the presence of 65 mM 3-AT. GFP was used as a negative control.

(B) *In vitro* pulldown assay to examine the interaction between *At*MED25 and RAP2.2/RAP2.12. Purified *in vitro* expressed proteins were used (FLAG-*At*MED25Δq [lacking the Q-rich motif], RAP2.2-CFP and RAP2.12-CFP). *At*MED25 was expressed without the glutamine-rich Q-motif to facilitate protein synthesis. GFP affinity beads were used for the pull-down assay. Anti-GFP and anti-FLAG antibodies were used to detect respective fusion proteins. As input control, 10% of the protein samples was loaded. As negative IP control, FLAG-*At*MED25Δq was loaded onto the GFP affinity beads (lane 5).

(C) Nuclear localisation of *At*MED25-GFP in leaves of stable transgenic Arabidopsis plants under normoxia and after 3 h of hypoxia, respectively. Nuclei were stained with 4′,6-diamidino-2-phenylindole (DAPI). Scale bar: 20 μm.

(D) Bimolecular fluorescence complementation assay of the interaction between *At*MED25 and ERFVIIs. *At*MED25-nYFP and RAP2.2-cYFP or RAP2.12-cYFP or the negative control empty vector (EV)-cYFP constructs were co-transformed into Arabidopsis protoplasts to detect protein–protein interaction *in vivo*. YFP fluorescence indicates protein complex formation in nuclei, which were stained with DAPI. As a negative control, RAP2.2-cYFP and RAP2.12-cYFP were tested against nYFP EV. At least 20 cells were analysed. Scale bar: 5 μm.

(E) Yeast two-hybrid analysis between *At*MED25 and RAP2.12 to map the interaction domain of RAP2.12. Cloned RAP2.12 fragments are indicated on the left together with positions of conserved motifs (Nakano et al., 2006). Protein interactions were tested on SD−LWH in the presence of 65 mM 3-AT. GFP was used as a negative control.

facilitates Mediator complex association with stress-related transcription factors (Yang et al., 2014). Specific binding to stress-related transcription factors has already been reported for several of the subunits tested (He et al., 2021; Zhang et al., 2014). However, none of the subunits could bind to RAP2.2 or RAP2.12 (Figure S1), suggesting

*At*MED25 is the sole component physically linking these ERFVII factors to the Mediator complex.

To narrow down regions within RAP2.12 mandatory for *At*MED25 binding, truncated transcription factor proteins lacking individual domains were generated (Figure 1E). Several domains conserved in ERFVII factors

execute important functions, including oxygen-dependent regulation of protein stability (CMVII-1), DNA binding (AP2 domain), and, in the case of RAP2.2 and RAP2.12, transactivation activity (CMVII-5) (Bui et al., 2015; Nakano et al., 2006). In yeast, N-terminus-specific protein fragments of RAP2.12 containing one or multiple conserved motifs upstream of the AP2 domain, that is, CMVII-1, CMVII-2, CMVII-3 and CMVII-6, failed to bind to *At*MED25. Likewise, C-terminal protein sequences spanning CMVII-4, CMVII-5, CMVII-7 and CMVII-8 were insufficient for interaction. In contrast, the middle part of RAP2.12 (amino acid 93–253) containing the AP2 domain with the adjacent upstream domain (CMVII-3) and a downstream flanking sequence was capable of *At*MED25 binding (Figure 1E). In conclusion, RAP-specific protein sequences required for *At*MED25 interaction (i.e. the AP2 domain and adjacent regions) are non-identical with domains linked to transactivation activity (Bui et al., 2015). Whilst the AP2 domain is highly conserved amongst ERFVII transcription factors (Figure S2a), the adjacent sequences are only similar between RAP2.2 and RAP2.12 in Arabidopsis and may enable interaction with *At*MED25. Especially the sequence upstream of the CMVII-3 motif appears to be solely present in both RAP-factors (Figure S2a). A protein–protein–DNA complex structure prediction using the AlphaFold3 server (Abramson et al., 2024) indicated that the AP2 domain flanking sequences of RAP2.12 interact with the ACID domain of *At*MED25 (Figure S2b), supporting our domain mapping results.

*At*MED25 confers low-oxygen tolerance by modulating transcriptional reprogramming under stress

Physical interaction of *At*MED25 with the two ERFVII transcription factors acting as key regulators of transcriptional responses and physiological tolerance towards hypoxia (Hinz et al., 2010; Licausi et al., 2011) suggests the involvement of *At*MED25 in plant tolerance to hypoxia. Stress tolerance of two independent T-DNA insertion lines lacking a functional *At*MED25 – med25-1 (*pft1-2*, SALK_129555; Kidd et al., 2009) and med25-2 (SALK_080230; Xu & Li, 2011) (Figure 2A; Figure S3) – was tested by subjecting respective seedlings to anoxia (Figure 2B,C). Both mutants showed a decreased survival score and thus reduced low-oxygen tolerance compared to the stressed wildtype. Under non-stress conditions, no difference to wildtype seedlings in terms of growth was visible (Figure 2B). However, at the age of 6 weeks, *med25* plants possessed slightly lower rosette size and dry weight (Figure 2D,F). Hence, to reliably compare performances of adult mutant and wildtype plants under dark submergence, stress-specific biomass accumulation relative to control conditions was calculated in addition to absolute plant weight. Both *med25-1* and *med25-2* plants exhibited stress-sensitive phenotypes with a stronger reduced relative fresh

and dry weight than the submerged wildtype (Figure 2E,F), indicating *At*MED25 confers low-oxygen stress tolerance during seedling and vegetative stages.

As *At*MED25 interacts with ERFVII factors involved in transcriptional reprogramming under low-oxygen stress, we hypothesised that *At*MED25 may affect transcriptional responses to hypoxia. To test this hypothesis, we performed RNA-seq analysis with *med25-1* and wildtype seedlings under normoxic and short-term hypoxic conditions (3 h, 1% O_2). Under normoxic conditions, 2042 differentially expressed genes (DEGs, false discovery rate [FDR] ≤0.05 and $\log_2$ fold change [FC] ≥1 or ≤−1) were identified, as indicated in Data S1. A gene ontology (GO) enrichment analysis revealed that genes involved in the response to stress, especially biotic stress, were upregulated in *med25-1* under control conditions (Data S1). This observation aligns with a reported increased basal pathogen tolerance of *med25* mutants in rice and Arabidopsis (Blomberg et al., 2023; Suzuki et al., 2022). Amongst the downregulated DEGs, mainly genes involved in cell wall-related processes were present, suggesting altered development or cell wall composition. Upon hypoxia, 758 DEGs were identified in the wildtype, whilst in *med25-1*, 543 DEGs were found (Data S1). In the wildtype, 440 genes were induced, whilst in *med25-1*,293 genes responded, indicating for the latter an overall weaker transcriptional response to hypoxia. GO enrichment for genes significantly responding in the wildtype (group I) but not in *med25-1* upon hypoxia was mainly related to biotic stress, drought, wounding and ABA (Data S2). Several HCGs, characterised by their strong upregulation under hypoxia (Mustroph et al., 2009), were found amongst the overlapping 125 upregulated genes (group II, Figure 2G; Data S2). However, in general, HCGs responded weaker in the *med25-1* mutant as compared to the wildtype (Figure 2H; Figure S4). *PDC1, HRA1, PCO1, PCO2, HYPOXIA UNKNOWN PROTEIN 9* (*HUP9*) and *HRE2* were amongst HCGs being lower expressed in *med25-1*, whilst *PHYTOGLOBIN 1* (*PGB1*) and *ETHYLENE RESPONSE 2* (*ETR2*) showed similar expression levels as in the wildtype. Genes only responding to hypoxia in *med25-1* (group III) showed a GO enrichment for trehalose metabolism. Not only were fewer genes induced in *med25-1* as compared to the wildtype but also fewer were downregulated (250 vs. 318, respectively) (Figure 2G,H). Group IV represents genes significantly downregulated in the wildtype under hypoxia, amongst them genes encoding membrane-related proteins (Data S2). Commonly downregulated genes (group V) comprised genes regulating cell wall organisation and biogenesis. In addition, 89 genes (group VI) were only downregulated in the stressed *med25-1* mutant, however, no significantly enriched GO term could be obtained. Taken together, *At*MED25 has a profound role in the transcriptional response to low-oxygen stress in Arabidopsis.
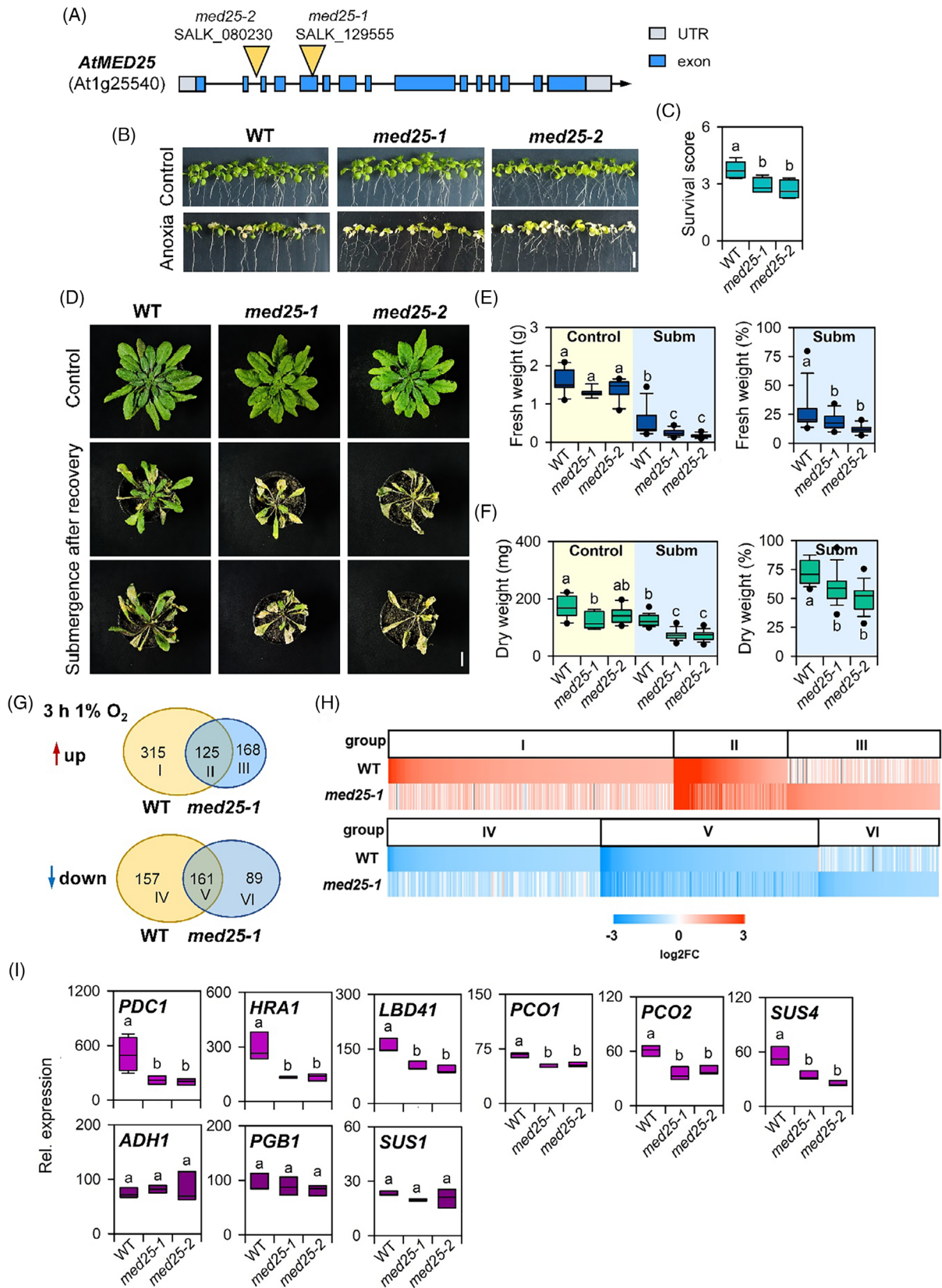
Figure 2. *At*MED25 is a positive regulator of low-oxygen stress adaptation.
(A) Schematic representation of T-DNA insertion lines *med25-1* (SALK_129555) and *med25-2* (SALK_08230). The location of the insertion site is indicated (yellow arrowhead).
(B) Phenotypes of *med25-1* and *med25-2* and wildtype (WT) seedlings after 9 h anoxia treatment (0% O_2) followed by 3 days of recovery. Scale bar: 1 cm.
(C) Anoxia survival scores of *med25* mutants and WT seedlings. $n = 5$ (with 15 seedlings/genotype). Different letters above boxes indicate significant differences to WT (one-way ANOVA, $P < 0.05$).
(D) Phenotypes of 6-week-old *med25-1* and *med25-2* and the WT after submergence. Scale bar: 2 cm.
(E, F) Fresh weight (E) and dry weight (F) of WT, *med25-1* and *med25-2* plants (given as absolute and relative values) under control conditions ($n = 8$) or after exposure to dark submergence for 3 days followed by a 5 days recovery ($n = 19$). Different letters above bars indicate significantly different groups (one-way ANOVA, $P < 0.05$).
(G) Venn diagrams of an RNA-Seq analysis for WT and *med25-1* plants under hypoxic conditions (3 h with 1% O_2). Up- and downregulated responses are presented separately ($n = 3$).
(H) Heatmaps indicate clustered and grouped (I–VI) up- or downregulated genes upon hypoxia in the WT and *med25-1*. Data for heatmaps are given in Data S1 and S2.
(I) Hypoxia core gene (HCG) expression after 3 h of hypoxia in WT, *med25-1* and *med25-2*. Boxes indicate relative fold change (FC) compared to normoxia ($n = 5$), as determined by RT-qPCR. Different letters above boxes indicate significantly differently expressed genes (one-way ANOVA, $P < 0.05$).

Induction of a subset of ERFVII target genes under hypoxia is *At*MED25-dependent

The ERFVII transcription factors RAP2.2 and RAP2.12 are the principle regulators of HCG expression (Gasch et al., 2016) and shown to interact with *At*MED25. Next to RNA-seq analysis, we validated the impaired HCG induction in *med25-1* and *med25-2* plants upon hypoxia using real-time quantitative polymerase chain reaction (RT-qPCR) (Figure 2I). Whilst a 3 h exposure to 1% oxygen resulted in strong induction of ERFVII-controlled hypoxia-responsive genes in wildtype plants, induction was compromised for the genes *PDC1*, *HRA1*, *LOB DOMAIN-CONTAINING PROTEIN 41* (*LBD41*), *PCO1*, *PCO2* and *SUCROSE SYNTHASE 4* (*SUS4*) in both *med25* mutants (Figure 2I). Notably, in contrast to these genes, *ADH1* and *PGB1*, but also *SUS1* remained unaffected in their responses to hypoxia in *med25* plants (Figure 2I), indicating ERFVII-regulated HCGs group into *At*MED25-dependent and -independent genes.
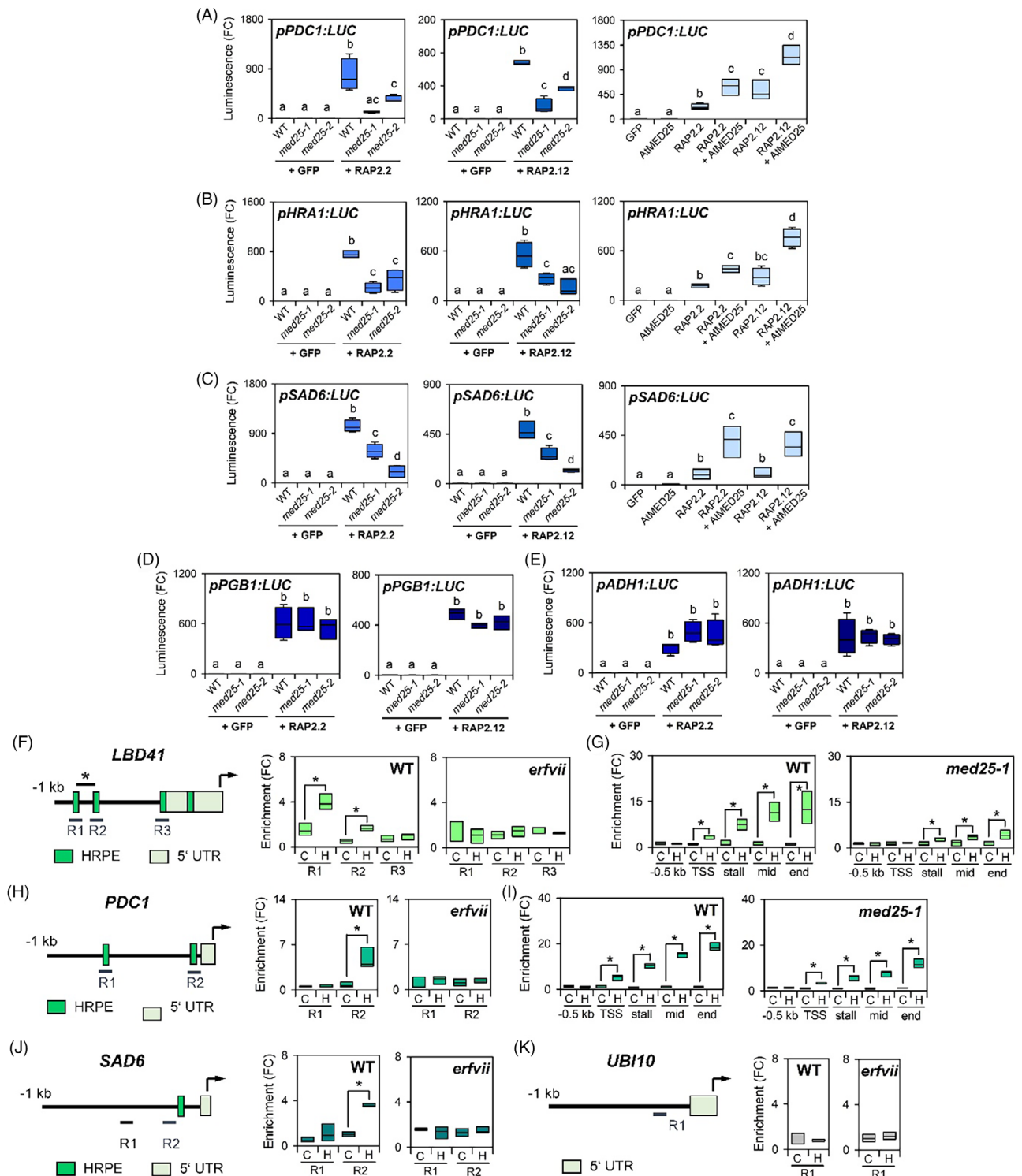
Physical interaction of *At*MED25 with RAP2.2 and RAP2.12 (Figure 1A,B,D) and the role of *At*MED25 in regulating ERFVII-dependent gene expression and physiological low-oxygen tolerance (Figure 2B–F,I) led us to test the transcriptional activity of RAP2.2 and RAP2.12 in the presence and absence of *At*MED25, respectively. For this, in addition to the wildtype, transactivation assays were performed in *med25-1* and *med25-2* knock-out backgrounds (Figure 3A–E). Induction of luminescence-based reporter constructs comprising the promoters of *PDC1* (Figure 3A), *HYPOXIA-RESPONSE ATTENUATOR 1* (*HRA1*, Figure 3B) and *STEAROYL-ACYL CARRIER PROTEIN Δ9-DESATURASE 6* (*SAD6*) (Figure 3C) by RAP2.2 and RAP2.12 was compromised in the absence of *At*MED25 and increased upon *At*MED25 co-expression, respectively. In contrast, induction of *pADH1:LUC* or *pPGB1:LUC* reporters by RAP2.2 and RAP2.12 in *med25* protoplasts was unaffected upon loss of *At*MED25 (Figure 3D,E), being in line with *ADH1* and *PGB1* similarly responding to hypoxia in *med25* knock-out mutants and the wildtype (Figure 2I). Taken together,

*At*MED25 is required for the regulation of a subset of ERFVII-controlled genes under stress.

*At*MED25 association with ERFVII-regulated promoters requires hypoxia

To investigate the dynamics of *At*MED25 association with ERFVII-regulated promoters, chromatin immunoprecipitation quantitative PCR (ChIP-qPCR) was conducted using plants expressing GFP-tagged *At*MED25 as bait (Figure 3F–J). Next to aerobic conditions, *At*MED25-promoter interactions were studied after 3 h of hypoxia, which is the time point where ERFVII factors such as RAP2.12 are detectable in the nucleus (Kosmacz et al., 2015). *At*MED25 enrichment at genomic DNA spanning different promoter regions of the tested hypoxia-inducible genes *PDC1*, *LBD41* and *SAD6* was analysed. These promoter regions were selected because they contain or are closely located to an HRPE copy previously shown to be recognised by RAP2.2 and RAP2.12 (Gasch et al., 2016). Significant enrichment of *At*MED25 on HRPEs-containing promoter regions of *LBD41* (Figure 3F), *PDC1* (Figure 3H) and *SAD6* (Figure 3J) occurred under hypoxia but not under aerobic conditions, whilst for the negative control, *UBIQUITIN 10* (*UBI10*), no *At*MED25 enrichment was detectable under both conditions (Figure 3K). To validate that *At*MED25 association with hypoxia-responsive promoters depends on ERFVII factors, the *erfvii* quintuple mutant (Marín-de la Rosa et al., 2014) was included in our analyses. Unlike in the wildtype (Figure 3F–J), *At*MED25 failed to bind to hypoxic promoters in *erfvii* upon exposure to hypoxia (Figure 3F–J).

To determine if *At*MED25 is required for recruitment of RNAPII to hypoxia-inducible ERFVII-controlled genes, ChIP-qPCR assays were performed with wildtype and *med25-1* plants exposed to hypoxia or kept under control conditions using an RNAPII-specific antibody. Pulled-down DNA was quantified by qPCR at specific regions along two hypoxia-related genes to evaluate the potential enrichment of RNAPII occupancy on the DNA. As previously described

(Hemsley et al., 2014), the following regions were probed: (i) 500 bp upstream of the transcription start site (TSS − 500), (ii) the TSS site itself, (iii) 50 bp after the start codon (the site of RNAPII stalling if it occurs) and (iv) the middle region of the ORF and 3′UTR region (Figure S5). Under normoxic conditions, *LBD41* and *PDC1* were

Figure 3. *At*MED25 modulates ERFVII-dependent activation of hypoxia-responsive promoters.
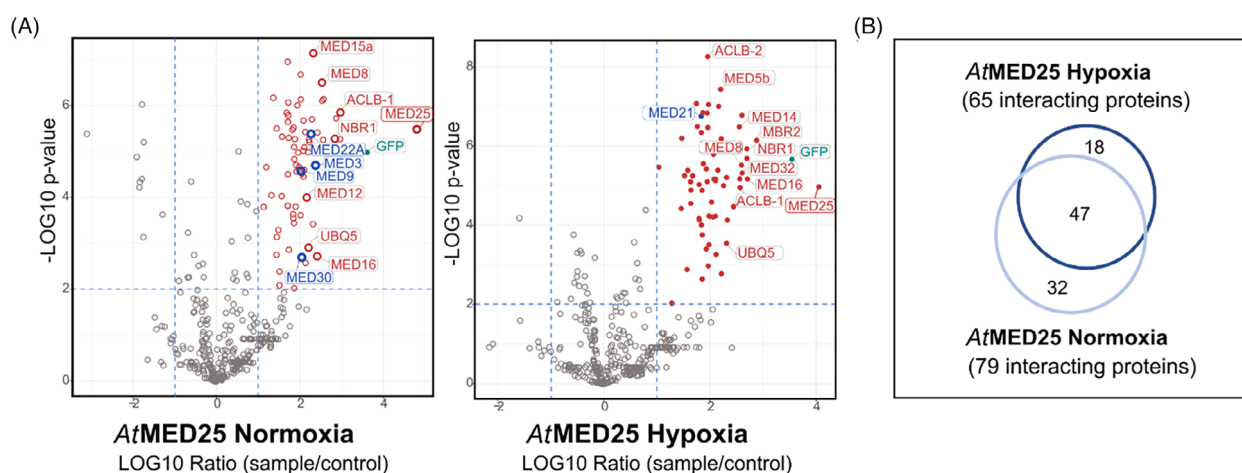(A–C) Activity of RAP2.2 and RAP2.12 on (A) *pPDC1:LUC*, (B) *pHRA1:LUC* and (C) *pSAD6:LUC* in protoplasts of wildtype (WT), *med25-1* and *med25-2* (left) and in WT protoplasts upon *AtMED25* co-expression (right).
(D, E) Unaffected activity of RAP2.2 and RAP2.12 on (D) *pPGB1:LUC* and (E) *pADH1:LUC* in protoplasts of WT, *med25-1* and *med25-2*. (A–E) $n = 4$. Different letters above bars indicate significantly different groups (one-way ANOVA, $P < 0.05$). A GFP construct was used as a negative control.
(F, H, J, K) ChIP assays with *At*MED25-GFP to assess *At*MED25 association with hypoxia-responsive promoters in WT and *erfvii* backgrounds. (F) *LBD41*, (H) *PDC1*, (J) *SAD6*, and (K) *UBI10*, the latter serving as negative control. Schemes indicate upstream genomic regions (R), and the presence of the HRPE motif (green box). The position of the *LBD41* HRPE motif, bound by RAP2.2 and RAP2.12 (Gasch et al., 2016) is indicated. $n = 3$. Asterisks in the graphs indicate significant enrichment (one-way ANOVA, $P < 0.05$).
(G, I) RNAPII recruitment to *LBD41* and *PDC1* promoters in WT and *med25-1* background under control and hypoxic conditions (3 h 1% O₂). Map of primer pair locations along the two genes is provided in Figure S5. ChIP enrichment at each location is referenced to negative control samples (−antibody controls). Values were calculated using the ΔΔC$_T$ method. $n = 3$. Asterisks in the graphs indicate significant enrichment (one-way ANOVA, $P < 0.05$).

transcriptionally almost undetectable and no significant enrichment for RNAPII along the genomic region was identified (Figure 3G,I). However, upon hypoxia, a significant enrichment for RNAPII was observed in the wildtype for both *LBD41* and *PDC1* (Figure 3G,I). In comparison to the wildtype, a considerably weaker enrichment for RNAPII occurred in *med25-1* showing that *At*MED25 modulates the transcriptional upregulation of a distinct set of hypoxia-responsive genes regulated by ERFVIIs.

*At*MED25 interactome is altered under oxygen constraints

The Mediator complex represents a highly flexible protein structure able to adjust dynamically to environmental signals in terms of its subunit composition, abundance and stability (Dolan et al., 2017). Also, the ability of individual subunits to conditionally interact with other Mediator complex components or proteins with different functions, for example, transcription factors, partially depends on environmental stimuli (He et al., 2021). We investigated if oxygen shortage affects the *At*MED25 interactome to reveal hints towards the response of the Mediator complex as a whole to hypoxia. To test this, we performed immunoprecipitation using GFP-tagged *At*MED25 in Arabidopsis and conducted mass spectrometry analysis (immunoprecipitation coupled to mass spectrometry [IP-MS]) to reveal the condition-specific interactomes. Specifically, *35S:AtMED25-GFP* plants were stressed for 3 h (1% O₂) and the *At*MED25-interactome herein was compared with that of plants under non-stress conditions using three biological replicates (Figure 4A,B; Figure S7; Data S3). Under control and stress conditions, a multitude of co-purified proteins were identified. Amongst them, 47 proteins were detected under both conditions, suggesting that these *At*MED25 interaction partners associate independently with the actual oxygen availability. Amongst the constitutively interacting proteins were 16 Mediator subunits, such as *At*MED8, *At*MED11, *At*MED18, *At*MED16 and *At*MED32 belonging to the Head and Tail modules, respectively, as well as *At*MED12, *At*MED13 and CDKE belonging to the associated kinase module. Additionally, proteins with other molecular functions, including two *At*MED25-regulating E3 ubiquitin-protein ligases (MBR1 and MBR2; Iñigo

Figure 4. The *At*MED25 interactome identified by immunoprecipitation coupled to mass spectrometry (IP-MS) is conditional.
(A) Volcano plots display all identified proteins under normoxia and hypoxia after the IP-MS. The distribution of identified proteins is according to the Log fold change of average spectral counts and −Log₁₀ *P*-value. Significantly enriched proteins (false discovery rate <0.01) likely interact with *At*MED25 and are shown in colour (red: common for both conditions and blue: specific for one condition). The data presented is based on three biological replicates.
(B) Venn diagram showing the overlap in the identified interacting proteins under hypoxic and normoxic conditions.

et al., 2012) and two ELKS/Rab6-interacting/CAST family proteins (ELKS1 and ELKS2) were detected under both conditions. Solely under normoxia, 32 proteins were co-purified with AtMED25, including four Mediator subunits (AtMED3, AtMED9, AtMED22A and AtMED30), the kinases ARABIDOPSIS EL1-LIKE 1 (AEL1) and AEL3 and the ubiquitin-binding protein TOM1-LIKE 6 (TOL6). On the other hand, under hypoxia, 65 proteins co-purified with AtMED25, of which 18 proteins were only enriched under stress. Hypoxia-specific proteins included, next to the Mediator subunit AtMED21, also the RNA-binding protein ATRBP45C, the protein kinase RAF20 and the CCCH zinc-finger protein C3H44. Taken together, hypoxia appears to affect the AtMED25-interactome concerning other Mediator subunits but also functionally diverse proteins, suggesting that protein–protein interactions with AtMED25, but also the Mediator complex itself are changed upon hypoxia.

Amongst the Mediator subunits constitutively associated with AtMED25 in-planta were AtMED8 and AtMED16 (Figure 4A,B; Figure S7; Data S3). Additionally, a direct AtMED16–AtMED25 interaction was verified in the heterologous system yeast (Figure S6). Previously, it was shown that AtMED16 acts together with AtMED25 in the context of transcriptional adjustment to iron deficiency (Yang et al., 2014). Moreover, AtMED25 and AtMED16 synergistically initiate transcription mediated by the transcription factor ETHYLENE-INSENSITIVE 3 (EIN3). Of note, EIN3 associates directly with AtMED25 to control some ethylene-mediated transcript responses, whilst AtMED16 is incapable of physically binding to EIN3 (Yang et al., 2014). As reported for EIN3, we found that RAP2.2 and RAP2.12 interact with AtMED25, but not with AtMED16 (Figure S1). Next to that, also AtMED8 was reported to have cooperative functions with AtMED25 in promoting flowering time in Arabidopsis (Bäckström et al., 2007; Yuan et al., 2023). Because of the partially overlapping functions of AtMED8 and AtMED16 with AtMED25 under various conditions, they might also have roles in ERFVII-dependent transcriptional responses during hypoxia. Of note, since there is no physical interaction with RAP2.2 or RAP2.12 (Figure S1), the effects of AtMED8 and AtMED16 on transcription factor action, if any, are only indirect.

AtMED25 action under hypoxia does not require AtMED8 or AtMED16 and is ethylene-independent

To examine the potential contribution of AtMED8 and/or AtMED16 to low-oxygen stress tolerance, performances of med8 (He et al., 2021) and med16 (yid1, Yang et al., 2014) seedlings subjected to anoxia were studied. No difference in survival was detectable for both mutants as compared to the stressed wildtype (Figure 5A,B). As AtMED16 can physically interact with AtMED25, it potentially indirectly acts on ERFVII transcription factors. To test this, transactivation assays with RAP2.2 and RAP2.12 using med16 or wildtype protoplasts were performed. Additionally, ERFVII activities in the wildtype upon AtMED16 co-expression
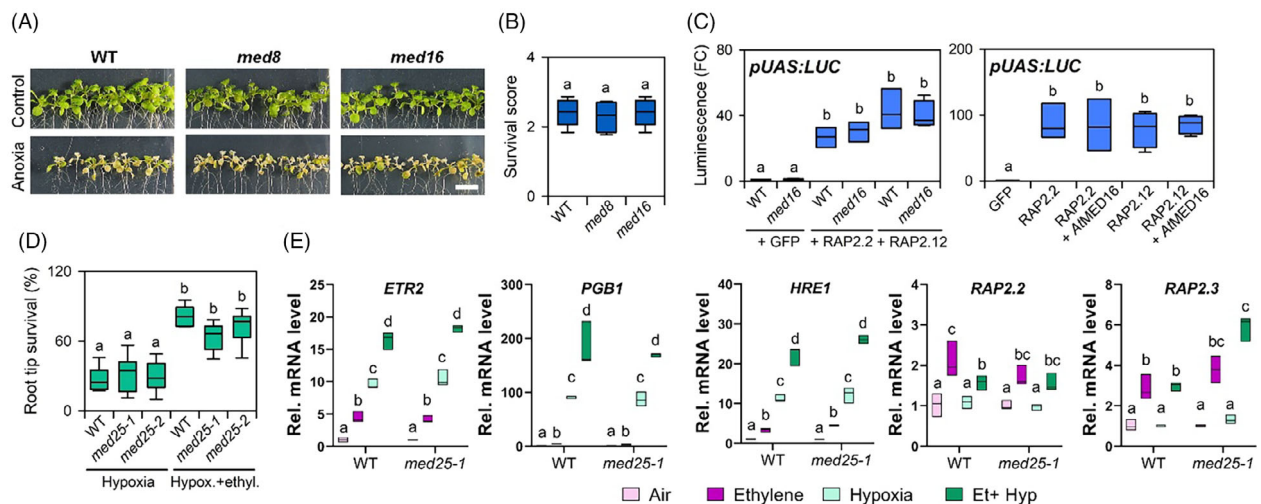

Figure 5. AtMED25-dependent transcript responses do not involve AtMED8, AtMED16 or ethylene.
(A) Phenotypes of med8, med16 and wildtype (WT) seedlings after 9 h anoxia treatment (0% O₂) followed by 3 days of recovery. Scale bar: 1 cm.
(B) Survival scores of med8 and med16 mutants and WT seedlings after recovering from anoxia treatment. $n = 5$ (with each 15 seedlings/genotype). Different letters above boxes indicate significant difference to WT (one-way ANOVA, $P < 0.05$).
(C) RAP2.2 and RAP2.12 activity on pUAS:LUC reporter in WT and med16 protoplasts (left) or in WT protoplasts upon AtMED16 co-expression (right). $n = 4$. Different letters above bars indicate significantly different groups (one-way ANOVA, $P < 0.05$). A GFP construct was used as a negative control.
(D) Relative root tip survival of hypoxia-treated (3.5 h) WT, med25-1 and med25-2 seedlings (18 rows containing approximately 23 seedlings/genotype/treatment) after 4 h of air/ethylene (5 ppm) pre-treatment. Different letters above boxes indicate significant difference to WT (one-way ANOVA, $P < 0.05$).
(E) Relative transcript abundance of ethylene-responsive genes in root tips of WT and med25-1 seedlings after air/ethylene (4 h) and subsequent hypoxia treatment (4 h). Boxes indicate the relative change of mRNA abundance as compared to air-treated control samples ($n = 3$ with every two technical replicates), determined by RT-qPCR. Different letters above boxes indicate significantly different values (two-way ANOVA, $P < 0.05$).

were analysed (Figure 5C). In *med16*, the transcriptional activities of ERFVIIs remained unaffected as compared to the wildtype. Likewise, co-expression of *AtMED16* could not increase transcription factor activity in wildtype protoplasts (Figure 5C). Combined, our data suggest that, unlike under other conditions, *At*MED25 does not act in concert with either *At*MED8 or *At*MED16 to mediate hypoxic responses involving ERFVII factors.

*At*MED25 (and *At*MED16) action in iron deficiency-related transcriptional responses involves the transcription factor EIN3 acting in an ethylene-dependent manner (Yang et al., 2014). Ethylene is a key phytohormone for plant adaptation to hypoxia through transcriptional, translational and proteolytic control of flooding-induced hypoxia responses (Cho et al., 2022; Liu et al., 2022). Ethylene promotes gene expression and survival under hypoxia partially by enhancing ERFVII stability, which is achieved by blocking NO-mediated ERFVII proteolysis by inducing the NO-scavenger PGB1 (Hartman et al., 2019). The lack of a need for cooperation between *At*MED25 and *At*MED16 under hypoxia (Figure 5A–C) suggests a limited participation of *At*MED25 in ethylene-mediated responses to hypoxia. Indeed, under oxygen constraints, *med25-1* and *med25-2* mutants benefitted, like the wildtype, from ethylene pre-treatment to improve hypoxia root tip survival (Figure 5D). The observed stimulation of mutant performance under hypoxia stress by ethylene indicates limited involvement of *At*MED25 in ethylene-mediated adaptation to hypoxia. In line with this, expression analysis of ethylene-treated *med25-1* and wildtype root tips showed similar induction of the ethylene-responsive genes *ETR2*, *PGB1*, *HRE1*, *RAP2.2* and *RAP2.3* (Figure 5E), further supportive of *At*MED25 functioning in ethylene-independent responses to low oxygen.

The ERFVII-MED25 module is functionally conserved in Arabidopsis and rice

The Mediator complex with its multi-module structure is conserved between eukaryotic organisms (Harper & Taatjes, 2018). Multiple sequence alignment of MED25 proteins from Arabidopsis and several agronomically important crop species, for example, rapeseed, soy, cotton, wheat, sorghum and rice revealed strong amino acid sequence conservation (Figure S8). Whilst *At*MED25 is most similar to *Br*MED25 from rapeseed, cereal MED25 proteins form an individual cluster, thereby separating them from dicot species (Figure S8a). Within the cereal clade, the activator-interacting domain (ACID) of *At*MED25, being sufficient for interaction with stress-induced transcription factors (Ou et al., 2011), is at the amino acid level nearly completely identical (Figure S8b,c). Hence, we tested whether RAP2.2 and RAP2.12 are capable of interacting with full-length *Os*MED25 from rice, which was indeed the case in yeast (Figure 6A). Moreover, the rice ERFVII transcription factor SUB1A, having a key regulatory

function in hypoxic responses and conferring tolerance to submergence (Locke et al., 2018; Xu et al., 2006), was capable of interacting with *At*MED25 as well as with *Os*MED25 (Figure 6A). It suggests that complex formation between ERFVIIs and MED25 proteins may represent a conserved feature in the regulation of low-oxygen responses in multiple plant species. To reveal whether *Os*MED25 acts as positive regulator of Arabidopsis ERFVII transcription factors, we tested RAP2.2 and RAP2.12 activities on different hypoxia-responsive target promoters. Induction of *PDC1-*, *HRA1-* and *SAD6*-specific luminescence-based reporters by both RAP2.2 and RAP2.12 was increased in the presence of *Os*MED25 (Figure 6B). Of note, in all assays performed, *Os*MED25 did not significantly affect target promoter activity in the absence of an ERFVII transcription factor. As SUB1A forms nuclear complexes with MED25 proteins in rice protoplasts (Figure 6C), the effect of *Os*MED25 on SUB1A performance on reporter constructs derived from the target promoters *OsERF66* and *OsERF67* (Lin et al., 2019) was investigated. This revealed a significant increase in SUB1A activity in the presence of *Os*MED25 (Figure 6D). These data combined indicate functional conservation of the MED25-ERFVII module in Arabidopsis and rice at the molecular level. To further demonstrate that MED25 proteins from both species have similar functions in adaptation to low-oxygen stress at the whole-plant level, the ability of ectopic *OsMED25* expression to restore wildtype performance of the Arabidopsis *med25-1* mutant was tested. For this, either *35S:OsMED25* or *35S:AtMED25* constructs were introduced into the mutant background and subsequent tolerance assays were performed (Figure 6E,F). The *med25-1/35S:OsMED25* seedlings subjected to anoxia showed a wildtype-like phenotype, that is, a higher survival score and thus higher tolerance than observed for *med25-1*, which was a comparable finding as for *35S:AtMED25*-complemented *med25-1* (Figure 6E,F). This indicates similar roles of MED25 from both species in establishing physiological resilience towards low-oxygen stress.

DISCUSSION

Plants, as all aerobic organisms, require oxygen for proper function and survival by generating respiratory energy. Environmental constraints can limit the amount of oxygen available to sustain plant metabolism and growth, especially during flooding events (Sasidharan et al., 2021). Upon submergence, several acclimation mechanisms are activated to minimise the detrimental effects of low oxygen. Whilst ERFVII factors are key regulators of transcriptional reprogramming during hypoxia (Gibbs et al., 2011; Hinz et al., 2010; Licausi et al., 2011; Xu et al., 2006), also other transcription factors have crucial roles in protecting plants from the harmful consequences of flooding stress (e.g. Eysholdt-Derzsó et al., 2023; Liu et al., 2021). In this study, we show that the Arabidopsis ERFVII factors RAP2.2 and
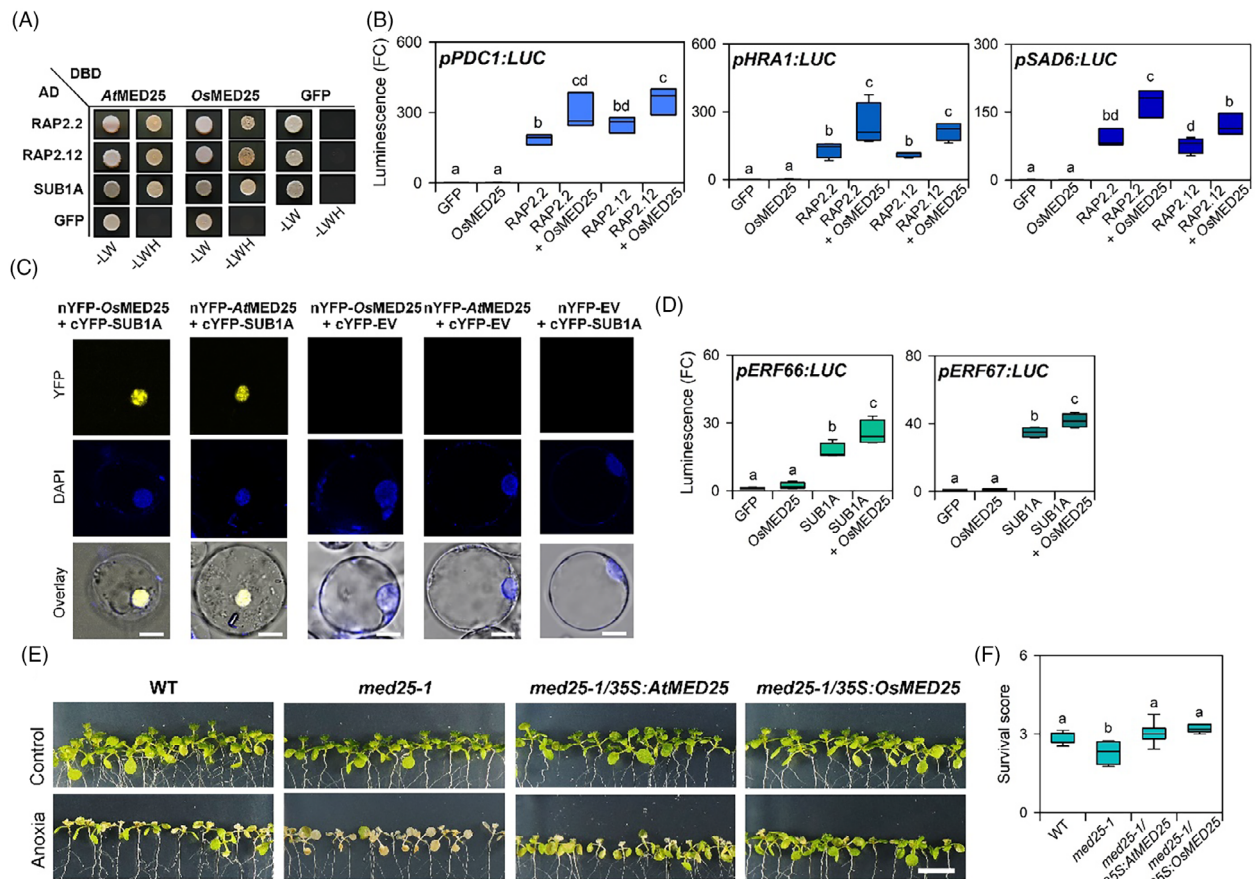
Figure 6. Functional conservation of the ERFVII-MED25 module in Arabidopsis and rice.

(A) Yeast two-hybrid assay with Arabidopsis and rice ERFVII factors combined with AtMED25 and OsMED25, respectively. Co-transfected yeast was selected on synthetic dropout (SD) medium lacking leucine and tryptophan (−LW). Protein interactions were tested on an SD medium lacking leucine, tryptophan and histidine (−LWH) in the presence of 65 mM 3-AT. GFP was used as a negative control.

(B) RAP2.2 and RAP2.12 activity on three reporter constructs in Arabidopsis wildtype (WT) protoplasts upon OsMED25 co-expression. $n = 4$. Different letters above bars indicate significantly different groups (one-way ANOVA, $p < 0.05$). A GFP construct was used as a negative control.

(C) Bimolecular fluorescence complementation assay using split-YFP with N-terminus of YFP fused to OsMED25 or AtMED25 and C-terminus to SUB1A. YFP signal indicates protein complex formation in nuclei, which were stained with 4′,6-diamidino-2-phenylindole (DAPI, blue). As negative controls, each tested construct was combined with the respective empty vector. Scale bar: 5 μm.

(D) SUB1A activity on pERF66:LUC (left) and pERF67:LUC (right) in rice WT protoplasts upon OsMED25 co-expression. $n = 4$. Different letters above bars indicate significantly different groups (one-way ANOVA, $P < 0.05$). A GFP construct was used as negative control.

(E) Phenotypes of WT, med25-1 and med25-1 complemented with either 35S:AtMED25 or 35S:OsMED25 after 9 h anoxia treatment (0% O_2) followed by 3 days of recovery. Scale bar: 1 cm.

(F) Survival scores of respective genotypes in (E) after recovering from the anoxia treatment. $n = 5$ (with each 15 seedlings/genotype). Different letters above boxes indicate significant difference to WT (one-way ANOVA, $P < 0.05$).

RAP2.12 interact with the Mediator complex through subunit AtMED25 to recruit RNAP II to promoters of a subset of hypoxia-responsive genes (Figure 7). Furthermore, we demonstrate that AtMED25 is required for submergence tolerance and that the composition of the Mediator complex attached to AtMED25 is modulated under low-oxygen stress. In addition, OsMED25 from rice is able to interact and promote the transcriptional activity of SUB1A in rice protoplasts. These results indicate that the potentially conserved MED25-ERFVII module enables plants to fine-tune their low-oxygen response to promote their survival.

In Arabidopsis, ERFVII family members have been shown to have partially overlapping and additive functions under hypoxia (Gasch et al., 2016; Zubrycka et al., 2023), whereby especially RAP2.2, RAP2.3 and RAP2.12 induce the expression of HCGs. Here, we found that out of the five ERFVIIs only RAP2.2 and RAP2.12 interact with AtMED25 (Figure 1A). Specifically, RAP2.12 interaction with AtMED25 is enabled by a transcription factor region containing the DNA-binding domain and its flanking regions (Figure 1E) and does not require the well-known C-terminal CMVII-5 domain essential for transcriptional activity (Bui et al., 2015). Interestingly, multiple sequence alignment (Figure S2a) revealed that RAP2.2, RAP2.12, but also SUB1A in rice share similar AP2-flanking regions, which are not found in the Arabidopsis ERFVII factors RAP2.3,
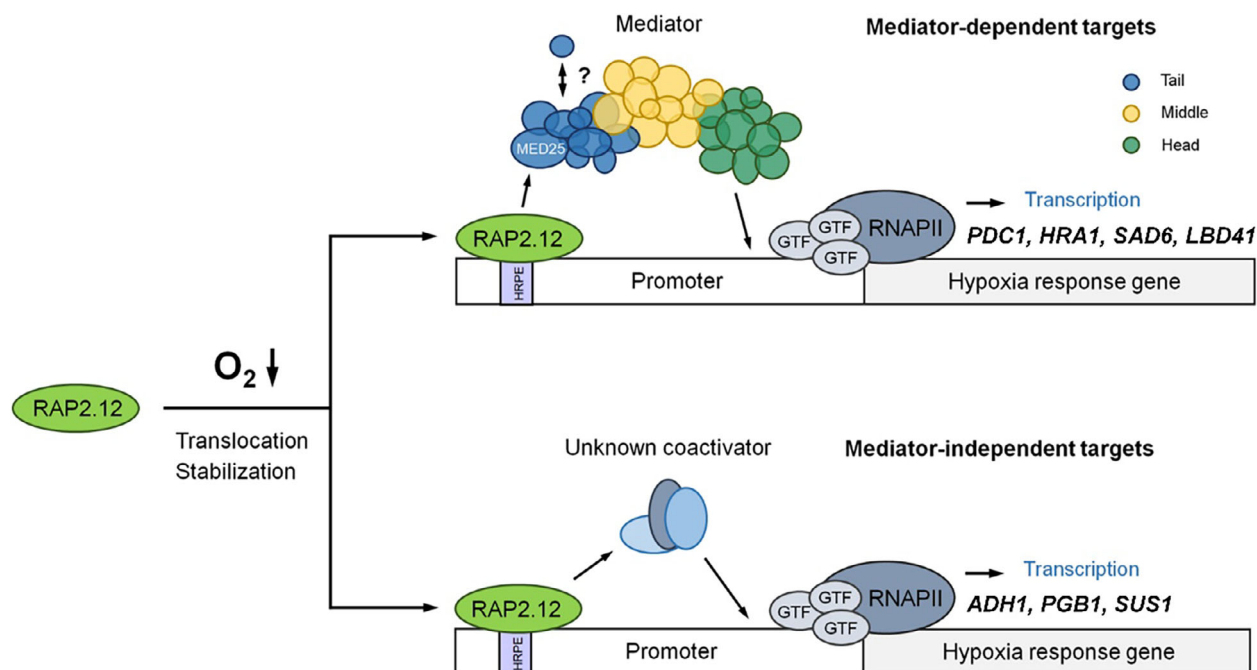
Figure 7. Proposed role of *At*MED25 action in ERFVII-dependent gene regulation under low-oxygen stress.
ERFVII transcription factors RAP2.2 and RAP2.12 associated with the HRPE motif present in the promoters of target genes such as *PDC1* and *LBD41*. Both ERFVII factors recruit the Mediator complex through an interaction with the Tail-specific *At*MED25 subunit. Association of *At*MED25 with ERFVII target promoters occurs under hypoxia only, likely through low-oxygen-induced accumulation of ERFVIIs in the nucleus. The ability of *At*MED25 to interact with other proteins is affected in an oxygen-dependent manner. Initiation of hypoxic gene transcription upon recruitment of RNAPII results in hypoxia tolerance. Similar to Arabidopsis, rice SUB1A can recruit *Os*MED25, suggesting that the ERFVII-MED25 module is functionally conserved in the plant kingdom.

HRE1 and HRE2 incapable of binding to *At*MED25. Together with the AlphaFold3-assisted modelling approach (Figure S2b), it can be assumed that these adjacent regions up- and downstream of the AP2 domain combined with the AP2 domain itself enable interaction with this Mediator subunit. *At*MED25 interacts with specific members of diverse transcription factor families, including the AP2/ERF family (Çevik et al., 2012; Ou et al., 2011), bHLH members (Çevik et al., 2012), bZIP proteins (Chen et al., 2012), MYB family members (Çevik et al., 2012) and several AUXIN RESPONSE FACTOR (ARF) proteins (Ito et al., 2016). As found for ERFVII factors in the current study, also in DREB2A the protein domain required for *At*MED25 interaction does not correspond to the transcriptional activation domain (Elfving et al., 2011). This suggests that the separation of the *At*MED25-interaction domain from the transcriptional activation domain might be a common feature in AP2/ERF proteins. In contrast, the VIRUS PROTEIN 16 (VP16) transcriptional activation domain directly interacts with the ACID domain of human MED25 (Vojnic et al., 2011), indicating that MED25 proteins might bind to some proteins directly via their transcriptional activation domains. Improved understanding of the interaction modes between *At*MED25 and the diverse transcription factors will greatly advance our understanding of transcriptional regulation in plants.

The Mediator complex acts as an information hub that conveys signals from transcription factors to RNAPII to modulate gene expression to guide development and secure plant survival (Agrawal et al., 2021). In response to environmental cues, the Mediator complex adopts different conformations and interacts with different regulatory factors to ensure context-specific transcriptional outcomes (Richter et al., 2022). *At*MED25 appears to act as a crucial component under stress since it is involved in various developmental and stress signalling pathways (Deng et al., 2023; Kazan, 2017; Zhai et al., 2020). Physical interaction of *At*MED25 with RAP2.2 and RAP2.12 suggests a role of *At*MED25 in low-oxygen tolerance in Arabidopsis. Indeed, we provide evidence that loss of *At*MED25 decreases tolerance to low-oxygen conditions as demonstrated at the seedling and vegetative stage (Figure 2B–F). Moreover, transcriptional responses to short-term hypoxia were severely affected in *med25-1* (Figure 2G,H). Of note, several hypoxia-induced ERFVII target genes, mandatory for acclimation to low-oxygen stress, showed an impaired induction in *med25* mutants. These genes comprise *PDC1*, *HRA1*, *HUP7*, *HUP9*, *LBD41*, *PCO1*, *PCO2* and *SUS4* (Figure 2I). However, other HCGs like *ADH1*, *PGB1* and *SUS1*, which also contain an ERFVII-specific HRPE element in their promoters (Gasch et al., 2016), remain unaffected in their transcriptional response to hypoxia (Figure 2I).

RAP2.3 was previously shown to activate *ADH1*, *PDC1*, *SUS1* and *SUS4* (Papdi et al., 2015), suggesting that it acts in part redundantly to RAP2.2 and RAP2.12. However, RAP2.3 does not interact with AtMED25 (Figure 1A), which may explain why the response of some HCGs is not altered by the absence of AtMED25. Moreover, the ERFVII factor HRE2 is able to regulate a subset of the HRPE-containing HCGs (Lee & Bailey-Serres, 2019), adding to the explanation why hypoxia-induced expression of ERFVII target genes in *med25* is not fully lost. Alternatively, RAP2.2 and RAP2.12 might also recruit other coactivators in addition to AtMED25, as in the *med25* mutant the activity of both transcription factors was substantially impaired, but not completely abolished (Figure 3A–E). A screen for potential interactions with other Mediator components did not yield additional subunits binding to RAP2.2 or RAP2.12 (Figure S1). It would be of interest to identify other coactivators acting in concert with AtMED25-independent ERFVII factors, that is, RAP2.3, HRE1 and HRE2. In analogy to plants, the key transcriptional regulator under hypoxia in humans, HYPOXIA-INDUCIBLE FACTOR 1 (HIF1), partially cooperates with the Mediator complex, specifically the CDK8 unit, to regulate a subset of its target genes (Galbraith et al., 2013). However, other HIF1-regulated hypoxia-responsive genes require HIF1 interaction with the TIP60 coactivator complex (Perez-Perri et al., 2016). Recruiting different coactivators may support the dynamic modulation of HIF1-regulated transcription under hypoxia, and thus allow a context-dependent cellular and phenotypic response. A potentially similar palette of coactivators, which themselves are regulated by hypoxia signals and assist in ERFVII-dependent transcript regulation, may enable flexible adaptation to hypoxia in plants.

To study AtMED25 association with promoters of hypoxia-responsive genes controlled by ERFVII factors, a ChIP experiment was performed (Figure 3F–K). Under control conditions, no enrichment for AtMED25 at the promoters of *LBD41*, *PDC1* and *SAD6* was observed. However, under hypoxia, AtMED25 is associated with these hypoxia-responsive genes, indicating that the binding of AtMED25 to target promoters is conditional. Specifically, AtMED25 was enriched at promoter regions encompassing an HRPE copy, suggesting that its association is ERFVII dependent. Indeed, simultaneous loss of all five *ERFVII* genes as in the *erfvii* mutant (Marín-de la Rosa et al., 2014) abolished the binding of AtMED25 to promoters under low-oxygen stress (Figure 3F,H,J). The stabilisation and translocation of ERFVII factors under hypoxia is an essential pre-requisite to enable AtMED25-promoter association upon stress. However, as the Mediator complex is highly dynamic and its conformation and composition are rapidly adjusted upon specific stimuli (Richter et al., 2022), the additional possibility exists that hypoxia, next to regulating ERFVII factors, also promotes the formation of a specific configuration of

the Mediator complex. Previously, Mediator complex modulation under stress through posttranslational modifications has been reported (Miller et al., 2012). Moreover, in the case of AtMED25, subunit regulation at the level of protein abundance has been demonstrated in the context of flowering time (Iñigo et al., 2012).

To investigate if, upon hypoxia, the function of AtMED25 is dynamically regulated, protein complexes containing AtMED25 under control and stress conditions were isolated and identified. Under control (normoxic) conditions, this protein pulldown resulted in 79 enriched proteins, whilst for hypoxia 65 proteins were identified; 47 proteins were shared by both conditions. Thus, hypoxia seems to impact the configuration of protein complexes containing AtMED25. Whilst most of the identified interacting Mediator subunits were shared between control and hypoxic conditions, AtMED21 was only associated with AtMED25 under hypoxia (Figure S7). Notably, AtMED21 is part of the Middle module of the Mediator complex enabling RNAPII association with the Mediator complex to promote transcription of target genes (Huang et al., 2021; Sato et al., 2016). Moreover, AtMED21 is recognised by the co-repressor TOPLESS to dampen transcriptional activation (Leydon et al., 2021), suggesting that AtMED21 acts as a key subunit in transcriptional regulation. Specific incorporation of AtMED21 into AtMED25-specific protein complexes suggests the formation of an active Mediator complex under hypoxia. Potentially, this complex formation might rely on the interaction between ERFVII factors and AtMED25. However, the inherent low abundance of transcription factor proteins limited their detection in our IP-MS approach. Investigating the function of AtMED21 in hypoxia-related transcription deserves future investigations. Next to that, under hypoxia, the chaperone J3 is associated with AtMED25 (Figure S7), which was previously shown to promote heat and drought stress tolerance in Arabidopsis (Wang et al., 2021). Furthermore, the Raf-like MAP kinase kinase kinase RAF20 only interacted with AtMED25 under hypoxia (Figure S7). RAF20 is known to activate subclass I SUCROSE NON-FERMENTING-1-RELATED PROTEIN KINASES 2 (SnRK2s) as part of osmotic stress responses (Soma et al., 2020), which is also an aspect of submergence stress. Taken together, the AtMED25 interactome composition is modulated in an oxygen-dependent manner. Consistent with the hypoxia-induced adjustments of the Mediator complex in Arabidopsis, in yeast, hypoxia also affects the Mediator complex by causing a subcellular redistribution of multiple subunits, including MED2, MED4 and MED9, from the nucleus to the cytosol (Henke et al., 2011). Interestingly, these subunits return to the nucleus during reoxygenation, indicating that the Mediator complex itself is receptive to low-oxygen signals and actively changes its composition. In analogy, our pulldown study revealed four Mediator subunits (AtMED3,

*At*MED9, *At*MED22A and *At*MED30), which only associate with *At*MED25 under normoxia, but not under hypoxia.

*At*MED25 reportedly cooperates with *At*MED16 to control the transcription factors EIN3 and ETHYLENE-INSENSITIVE3-LIKE 1 (EIL1) as part of iron deficiency responses (Yang et al., 2014), whilst in tomatoes, MED25 regulates fruit ripening through modulation of ethylene-dependent pathways (Deng et al., 2023). Next to that, *At*MED25 and *At*MED8 are both required for regulating transcriptional changes upon glucose treatment (Seguela-Arnaud et al., 2015). In our study, both *At*MED8 and *At*MED16 were identified as components of the *At*MED25-specific interactome (Figure S7). Although both subunits do not directly interact with RAP2.2 and RAP2.12 (Figure S1), their potential contribution to low-oxygen tolerance, partially due to the link to ethylene, was examined. In contrast to *At*MED25, *At*MED8 and *At*MED16 are dispensable for anoxia tolerance (Figure 5A,B). In line with that, the transcriptional activity of RAP2.2 and RAP2.12 towards hypoxia-responsive promoters was not impaired in the *med16* background (Figure 5C). As *At*MED25 is linked to the regulation of EIN3 and EIL1 (Yang et al., 2014), it was tested if it also participates in ethylene-mediated adaptation to hypoxia. Interestingly, *At*MED25 is not mandatory for ethylene-mediated root tip survival (Figure 5D), indicating that ethylene-mediated hypoxia acclimation acts through ERF-VIIs, but not *At*MED25. Fitting with this, transcript levels of ethylene-inducible genes were comparable in *med25-1* and the wildtype pre-incubated with ethylene and subsequently exposed to hypoxia (Figure 5E).

The MED25 subunit is conserved in plants, suggesting that the observed role in Arabidopsis in hypoxia adaptation may also be important for other species. As demonstrated previously, in both *Physcomitrium patens* and Arabidopsis, MED25 promotes salinity tolerance (Elfving et al., 2011). Furthermore, MED25 from wheat complements phenotypic aspects of the Arabidopsis *med25-1* knock-out mutant, including delayed flowering and disease resistance (Kidd et al., 2009). Conservation of MED25 function and amino acid sequence within the plant kingdom suggests a common role in hypoxia signalling in plants (Figure S8). Here, we show that MED25 proteins from Arabidopsis and rice are capable of interacting with the ERFVII factors RAP2.2, RAP2.12 (both Arabidopsis) and SUB1A (rice; Figure 6A). Furthermore, *Os*MED25 promoted the activity of RAP2.2 and RAP2.12 towards target promoters, whilst it could also stimulate the activation of rice *ERF66* and *ERF67* by SUB1A (Figure 6B,D; Lin et al., 2019). We also demonstrated that *Os*MED25 functionally replaces *At*MED25 *in planta* by restoring low-oxygen tolerance of respectively complemented *med25-1* mutant plants (Figure 6E,F). How exactly *Os*MED25 stimulates SUB1A activity will contribute to our knowledge of ERFVII-dependent gene regulation under stress. Taken together,

our findings add a new facet to the mechanisms by which plants respond and adapt to low-oxygen stress at the molecular level. Potentially, the provided identification of the role of MED25 in low-oxygen adaptation could help to improve flooding stress resilience in crops.

EXPERIMENTAL PROCEDURES

Plant material

For all indicated experiments, wildtype plants with Columbia-0 background were used. The knock-out mutants *med25-1* (*pft1-2*, SALK_129555; Kidd et al., 2009) and *med25-2* (SALK_080230; Xu & Li, 2011) were described previously and genotyped by PCR with the following primers: 5′-ATGACTTAAGGCAGCACATGC-3′ (LP) and 5′-GTGCTTCTGTCAGCGATTTTC-3′ (RP) for wildtype allele detection in *med25-1*, and 5′-AGGTGTTGGCAATATGTGAG-3′ (LP) and 5′-CAACGCATTCATAAAGCAAT-3′ (RP) for wildtype allele detection in *med25-2*. Detection of mutated alleles was done by PCR with the primer 5′-ATTTTGCCGATTTCGGAAC-3′ combined with RP. Total RNA of wildtype, *med25-1* and *med25-2* seedlings was extracted via Trizol reagent (Invitrogen, Waltham, MA, USA) according to the manufacturer's instructions. The remaining DNA was destructed using the TURBO DNA-free™ Kit (Invitrogen) and cDNA was transcribed using the RevertAid First Strand cDNA Synthesis Kit (Thermo Fisher Scientific, Waltham, MA, USA). Semi-quantitative RT-PCR for *AtMED25* was done with a gene-specific primer (Table S1).

The knock-down line *med16* (*yid1*), *med8* mutant (SALK_092406) and *erfvii* mutant were described previously (He et al., 2021; Marín-de la Rosa et al., 2014; Yang et al., 2014).

Growth conditions and low-oxygen treatments

Tolerance to anoxia (0% O_2, 9 h) was tested for *med25-1*, *med25-2*, *med25-1/35S:AtMED25* and *med25-1/35S:OsMED25*. Seeds were sown out on MS medium containing 0.5% (wt/vol) sucrose, stratified for 48 h at 4°C and germinated at 21°C day/18°C night with a photoperiod of 16 h light (150 μmol m^{-2} sec^{-1}) and 8 h dark. Eleven-days-old-seedlings were exposed to a 100% nitrogen atmosphere in the dark. After recovery, the survival score was determined by scoring the seedlings per plate as dead, impaired or healthy (survival score of 1, 3 or 5 respectively) according to Gibbs et al. (2011). For submergence assays with 4-week-old *med25-1* and *med25-2* plants, seeds were sown out on soil, stratified for 48 h at 4°C and germinated at 21°C day/18°C night with a photoperiod of 16 h light and 8 h dark. Plants were submerged in water in the dark for 3 days followed by a 5-days recovery phase. For ethylene and hypoxia treatments, root tip tolerance assays and RT-qPCR on *in vitro* grown seedlings on agar plates, the same conditions and methods were used as reported previously (Hartman et al., 2019; Liu et al., 2022). Briefly, 5-day-old Arabidopsis seedlings were grown vertically on *in vitro* plates and treated in glass desiccators with air or 5 μL L^{-1} ethylene for 4 h, followed by 4 h of hypoxia (0% O_2) by flushing with nitrogen gas.

Cloning of constructs

For interaction studies in yeast, full-length *AtMED25* and *OsMED25* coding sequences in pENTR/D-TOPO (Invitrogen) were together with coding sequences of *AtMED8*, *AtMED16*, *AtMED19*, *AtMED21*, *AtMED28*, *AtMED32*, *AtMED34* and *AtMED36* (kindly provided in pENTR/D-TOPO by Prof. Li-Jia Qu, School of Life Sciences, Peking University, Beijing, China) recombined into pDEST32 (Thermo Fisher Scientific), possessing the GAL4 DNA-binding domain, as

bait constructs. *AtMED25* coding sequence, *RAP2.2* and *RAP2.12* full-length and truncated coding sequences as well as the *SUB1A* (derived from *O. sativa* subsp. *indica* cv IR40931-26) coding sequence were cloned into pENTR/D-TOPO and together with *HRE1*, *HRE2* and *RAP2.3* in pENTR/D-TOPO (kindly provided by Prof. Margret Sauter, Christian-Albrechts University, Kiel, Germany) recombined into pDEST22 (Thermo Fisher Scientific), possessing the GAL4 activation domain, as prey constructs.

Transactivation assays were conducted using *PDC1*, *SAD6*, *HRA1*, *ADH1* and *PGB1* promoters recombined into pGWL7,0 and *RAP2.2*, *RAP2.12* and *SUB1A* coding sequences into p2GW7,0 (Bui et al., 2015; Karimi et al., 2002). In addition, *RAP2.2* and *RAP2.12* coding sequences were recombined into the p35S-GBD-GW vector for use in the pUAS system (Weltmeier et al., 2006).

For BiFC analysis, *MED25* coding sequences from Arabidopsis and rice were recombined into pDH51-GW-YFPn, whilst full-length *RAP2.2*, *RAP2.12* and *SUB1A* coding sequences in pENTR/D-TOPO (Invitrogen) were recombined into pDH51-GW-YFPc (Zhong et al., 2008).

For *in vitro* pulldown experiments the coding region of *At*MED25Δq was fused N-terminally with a FLAG-tag by PCR with oligonucleotides containing restriction site overhangs for cloning into pF3A WG BYDV (Promega, Fitchburg, WI, USA). RAP2.12 C-terminally fused to CFP was previously established (Schmidt et al., 2018). Similarly, the coding sequence of RAP2.12 was C-terminally fused to CFP by PCR and cloned into pF3A WG BYDV.

All oligonucleotide sequences used for cloning of constructs are listed in Table S1.

Plant transformation

Full-length *AtMED25* and *OsMED25* coding sequences and the full-length *AtMED25* promoter were cloned into pENTR/D-TOPO (Invitrogen) and recombined either into pK7WG2 (*AtMED25* and *OsMED25* coding sequences; Karimi et al., 2002) or pK7FWG2 (only *AtMED25*) providing the 35S promoter (Karimi et al., 2002) or pKGWFS7 (*AtMED25* promoter; Karimi et al., 2002). After transformation into *Agrobacterium*, *35S:AtMED25* and *35S:OsMED25* were transformed into *med25-1*, *35S:AtMED25-GFP* into wildtype and *erfvii* and *pAtMED25:GUS* into wildtype plants using the floral dip method. Antibiotic-resistant T1 seedlings were identified and, in the case of AtMED25-GFP, tested for a present GFP signal by confocal microscopy analysis.

Interaction studies in yeast

Recombinant pDEST22 and pDEST32 vectors were co-transformed into the *Saccharomyces cerevisiae* strain PJ69-4a (James et al., 1996) using the LiAc method and successfully transformed yeast colonies were selected on solid SD medium lacking Trp and Leu. Subsequently, single colonies were grown overnight (30°C, 300 g) in a selective SD medium and 3 µl were spotted on SD medium lacking Trp, Leu and His and containing 65 mm 3-amino-1,2,4-triazole. As negative controls, recombinant pDEST22 or pDEST32 vectors were co-transformed with the corresponding counterpart containing GFP.

Transactivation assays and BiFC analysis

For testing ERFVII activity, *35S:RAP2.2*, *35S:RAP2.12* or *35S:SUB1a* were co-transformed with reporter constructs and the normalisation vector containing *35S:RLUC* into protoplasts according to Wu et al. (2009) and Schmidt et al. (2013). For some assays, in addition to the mentioned plasmids, *35S:AtMED25*, *35S:OsMED25* or *35S:AtMED16* in p2GW7,0 were additionally co-transformed. In the case

of the pUAS reporter system, *RAP2.2* and *RAP2.12* in the p35S-GBD-GW (Weltmeier et al., 2006) were co-transformed together with *pUAS:LUC*. For each construct, 5 µg per transformation was used. Dual luciferase assays (Promega) with four independent replicates were employed as reported previously (Schmidt et al., 2013) and emitted luminescence signals were quantified using the SYNERGY MX (BioTek, Winooski, VT, USA) plate-reader system. At least four biological replicates were used for each experiment.

To study interaction between *At*MED25 and RAP2.2 or RAP2.12 in Arabidopsis mesophyll protoplasts, *35S:AtMED25* in pDH51-GW-YFPn was co-transformed with either *35S:RAP2.2* or *35S:RAP2.12* in pDH51-GW-YFPc following the tape-Arabidopsis-sandwich protocol (Wu et al., 2009). The complex formation of SUB1A with *Os*MED25 or *At*MED25 was investigated using the pE-SPYNE-GW and pE-SPYCE-GW vectors (Walter et al., 2004) in rice shoot protoplasts (*O. sativa* subsp. *japonica* cv. Nipponbare) following the protocol of Schmidt et al. (2013). As negative controls, recombinant vectors were co-transformed with the corresponding counterpart containing GFP. For each construct, 5 µg were used.

In vitro pulldown assay

For the *in vitro* pulldown assay, FLAG-tagged *At*MED25 protein and CFP-tagged RAP2.2 and RAP2.12 proteins (Schmidt et al., 2018) were expressed using TNT SP6 High Yield Wheat Germ (Promega) following the manufacturer's instructions. Subsequently, expression mixtures were filled up with 500 µl binding buffer (50 mm Tris–HCl, 150 mm NaCl) and 250 µl of *At*MED25 samples were mixed with an equal volume of RAP2.2 or RAP2.12. The samples were placed on a rotator at 16°C for 2 h to allow for complex formation. Subsequently, 25 µl calibrated magnetic anti-GFP beads were added (Chromotek, Planegg/Martinsried, Germany), and the samples were incubated for an additional hour at 16°C. After this incubation, the beads were collected and washed five times with 500 µl washing buffer (50 mm Tris–HCl, 150 mm NaCl and 0.5% TritonX-100). Subsequently, beads were resuspended in laemmli buffer (with β-ME) and heated to 95°C for 5 min to elute and denature the proteins. Eluted and input samples were analysed by 10% sodium dodecyl sulfate polyacrylamide gel electrophoresis and immunoblotting with anti-FLAG antibody (Sigma-Aldrich, Burlington, MA, USA) and anti-GFP antibody (Roche, Basel, Switzerland).

Confocal microscopy

Imaging and analysis of GFP and YFP signals to detect protein localisation and interaction were performed using an LSM780 confocal microscope (Zeiss, Oberkochen, Germany). Wavelengths for fluorophore excitation and emission were 488 and 500–550 nm for GFP and 514 and 520–550 nm for YFP, respectively. Nuclei were stained using 4′,6-diamidino-2-phenylindole following the manufacturer's advice and excitation and detection were obtained at 405 and 425–465 nm, respectively. Chlorophyll autofluorescence was detected at 655–685 nm. For *At*MED25-GFP localisation in stable Arabidopsis plants, 2-week-old seedlings were analysed. The authors acknowledge the team of the Light Microscopy Technology Platform of the Faculty of Biology, Bielefeld University, Germany.

RT-qPCR analysis

Extraction of RNA, genomic DNA removal, cDNA synthesis and RT-qPCR analyses were performed as described previously (Schmidt et al., 2013). Four to five biological replicates were used for each experiment. *UBIQUITIN10* served as a reference gene according to Licausi et al. (2011). Calculation of relative transcript abundance was done using the comparative cycle threshold (CT)

method (Livak & Schmittgen, 2001). Oligonucleotide sequences used for expression analysis of hypoxic genes can be found elsewhere (Schmidt et al., 2018). For ethylene, hypoxia treatments and subsequent RT-qPCR on *in vitro*-grown seedling root tips, protocols were used as described previously (Hartman et al., 2019), using *ADENINE PHOSPHORIBOSYL TRANSFERASE 1* (*APT1*) as a reference gene. Oligonucleotide sequences for RT-qPCR expression analysis related to hypoxia combined with ethylene can be found in Table S2.

RNA-seq library preparation, sequencing and analysis

Global transcript responses to hypoxia (3 h, 1% oxygen) were analysed in 14-day-old *med25-1* and wildtype seedlings grown on horizontal half-strength MS plates containing 0.5% sucrose. For each genotype and treatment, three biological replicates were used. Total RNA was extracted using the NucleoSpin® RNA Plant kit from Macherey-Nagel according to the manufacturer's instructions. Contaminating genomic DNA was removed using the Turbo DNA-free kit from Ambion according to the manufacturer's instructions. Subsequently, RNA quality and integrity were assessed using a QIAxcel platform (Qiagen, Hilden, Germany). The TruSeq® Stranded mRNA sample preparation 96 rcx kit (Illumina™, San Diego, CA, USA) following the low sample protocol according to Illumina™ guidelines was used to construct the library using 2.5 μg of total RNA. After adapter ligation the libraries were quantified using PicoGreen® (Life Technologies™, Carlsbad, CA, USA). The library were pooled and the Kapa SYBR® FAST universal qPCR kit (Kapa Biosystems™, Wilmington, MA, USA) for Illumina sequencing was used to quantify the number of the amplifiable molecules. In addition, the average fragment size of the libraries was analysed using the Bioanalyzer® (Agilent Technologies™, Santa Clara, CA, USA). An Illumina HiSeq 1500 sequencer was used in the high throughput mode using the TruSeq® SBS Kit in a 50-cycle pair-end run to sequence the libraries. The base-calling was done by the Illumina software that controls the sequencer and the alignment (as well as the QC and read counting) was done with the CLC Genomics workbench using default settings. Transcriptome analysis was performed by means of CLC Genomics Workbench v.6 using the *A. thaliana* reference sequence (TAIR10) including DESeq2. The expression values were normalised using quantile normalisation and pair-wise statistical analyses comparing the treatments performed using FDR-corrected *P*-values based on Baggerley's test (Baggerly et al., 2003). RNA-seq data is deposited at NCBI's Gene Expression Omnibus (GEO; record number GSE130962).

ChIP-qPCR analysis

Chromatin immunoprecipitation experiments were essentially done as previously described (Kaufmann et al., 2010; Neuser et al., 2019). In brief, 0.7–0.8 g 2-week-old *35S:AtMED25-GFP* seedlings were vacuum-infiltrated with MC buffer containing 1% formaldehyde. After nuclei isolation, the samples were sonicated to share the chromatin. Subsequently, immunopurification was performed using anti-GFP agarose beads (Chomotek, Planegg/Martinsried, Germany) to enrich for *At*MED25-GFP-bound DNA fragments. In addition, a negative control (binding control agarose beads; Chromotek) and input control were used. Immunoprecipitated chromatin was eluted three times with 100 μl of ice-cold glycine buffer (0.1 M glycine, 0.5 M NaCl, 0.05% Tween-20 [pH 2.8]). Each eluate was buffered with 150 μl of Tris–HCl (pH 9.0) and subsequently pooled for each sample. After elution, samples were treated overnight with Proteinase K (Roche) at 37°C. The next day, the proteinase K treatment was repeated for 6 h at 65°C. The

enriched DNA samples were precipitated overnight with 2.5 vol. 100% ethanol, 1/10 of NaAc and 1 μl glycogen (Invitrogen) at −20°C. Finally, samples were cleaned-up using the QIAquick PCR Purification Kit (Qiagen, Hilden, Germany). Samples were eluted from the column in a 30 μl volume and analysed by RT-qPCR with specific primers (Table S3).

RNAPII ChiP analysis was done similarly as described above and previously (Hemsley et al., 2014), with a couple of modifications. A ChIP-grade antibody against Pol II C-terminal domain repeats (Ab5408; Abcam) was immobilised on MagnaChIP™ Protein A magnetic beads (Sigma-Aldrich). Both the wildtype as well as the *med25-1* mutant were used for the analysis under normoxic and hypoxic conditions. Primers used to amplify gDNA regions are provided in Table S3.

GO term enrichment analysis

Gene ontology term enrichment analysis was done using the agriGO v2.0 webtool (http://systemsbiology.cau.edu.cn/agriGOv2/; Tian et al., 2017). GO terms with an FDR ≤0.05 were considered enriched. Heatmaps were generated using the Multiple Experiment Viewer (MeV) software (Saeed et al., 2017).

Multiple sequence alignment

For the multiple sequence alignment of MED25 proteins from different species, sequences of homologous proteins were obtained from Phytozome v12.0 and aligned with Clustal X.

In-planta identification of *At*MED25 interacting proteins by IP-MS

An *At*MED25-GFP-specific pull-down was performed as previously described by Wendrich et al. (2017). Approximately 3 g of leaf material were harvested from each condition and genotype in triplicates and flash frozen. The three biological replicates were ground and homogenised in extraction buffer containing 50mM Tris–HCl, pH 7.5, 0.15M NaCl, 1 Protease inhibitor tablet/50 ml (Roche) and 1% (v/v) NP40. Protein extracts were sonicated to disrupt chromatin, diluted (NP40 diluted to 0.2%) and then centrifuged twice for 15 min at 18 000 *g*. After incubation for 2 h at 4°C, with anti-GFP-coated microbeads (μMACS; Miltenyi), protein extracts were applied on the μColumns (μMACS; Miltenyi), washed and then eluted. The elute was reduced with dithiothreitol, alkylated with iodoacetamide and digested with sequencing-grade Trypsin. The next day, the peptides were purified using the Bond Elut OMIX tips (Agilent Technologies). The sample concentration was determined, and an equal amount of peptides (600 ng) was injected and analysed by liquid chromatography–tandem mass spectrometry with a tandem UltiMate 3000 RSLCnano system in-line connected to an Orbitrap Fusion Lumos Tribrid mass spectrometer (Thermo Fisher Scientific). Raw files were processed with the MaxQuant software (1.6.9.0) as reported by He et al. (2021). "ProteinGroups" file from MaxQuant was used as input in an R-script, data were filtered, Label-Free Quantification intensities were LOG10 transformed and the lowest value was set as a detection threshold. Statistical *t*-test was performed and ratios and *p*-values were calculated (Data S3). Hereafter, each condition was tested pairwise, and differential proteins were defined as having a |log$_2$ FC| ≥1 and *Q* value ≤0.05, and should be detectable in all replicates.

ACCESSION NUMBERS

Sequence information from this article can be found in the Arabidopsis Genome Initiative database under the following accession numbers: *ADH1* (AT1G77120), *AEL1* (AT2G25760), *AEL3*

(AT3G03940), *AtMED11* (AT3G01435), *AtMED12* (AT4G00450), *AtMED13* (AT1G55325), *AtMED16* (AT4G04920), *AtMED18* (AT2G22370), *AtMED19* (AT5G12230), *AtMED21* (AT4G04780), *AtMED22A* (AT1G16430), *AtMED25* (At1g25540), *AtMED28* (AT3G52860), *AtMED3* (AT3G09180), *AtMED30* (AT5G63480), *AtMED32* (AT1G11760), *AtMED34* (AT1G31360), *AtMED36* (AT4G25630), *AtMED8* (AT2G03070), *AtMED9* (AT1G55080), *APT1* (AT1G27450), *ATRBP45C* (AT4G27000), *C3H44* (AT3G51120), *ELKS1* (AT1G03290), *ELKS2* (AT4G02880), *ETR2* (AT3G23150), *HRA1* (AT3G10040), *HRE1* (AT1G72360), *HRE2* (AT2G47520), *HUP9* (AT5G10040), *J3* (AT3G44110), *LBD41* (AT3G02550), *MBR1* (AT2G15530), *MBR2* (AT4G34040), *OsERF66* (LOC_Os03g22170), *OsERF67* (LOC_Os07g47790), *OsMED25* (LOC_Os09g13610), *SUB1A* (DQ011598), *PDC1* (AT4G33070), *PCO1* (AT3G10040), *PCO2* (AT5G39890), *PGB1* (AT2G16060), *RAF20* (AT1G79570), *RAP2.12* (AT1G53910), *RAP2.2* (AT3G14230), *RAP2.3* (AT3G16770), *SAD6* (AT1G43800), *SUS1* (AT5G20830), *SUS4* (AT3G43190), *TOL6* (AT2G38410), *UBI10* (AT4G05320).

AUTHOR CONTRIBUTIONS

JHMS, JTvD and RRS-S designed the research. KvB, LL, S Frohn, S Frings, TR, FA, KW, KS, SH, RS, DV and AM carried out experiments. GTSB, FVB, SH, JTvD, JHMS and RRS-S analysed and visualised the data. JHMS, AM and RRS-S wrote the manuscript, all authors edited the manuscript.

CONFLICT OF INTEREST STATEMENT

The authors declare no conflict of interest.

SUPPORTING INFORMATION

Additional Supporting Information may be found in the online version of this article.

Data S1. Transcriptome and GO term analysis of wildtype and *med25-1* plants under control and hypoxia.

Data S2. GO term analysis of specific and overlapping DEGs in wildtype and *med25-1* upon hypoxia.

Data S3. List of interactors of *At*MED25 identified by GFP pull-down experiments under normoxia and hypoxia.

Figure S1. Yeast two-hybrid assays for testing interaction between Mediator complex subunits with the ERFVII factors RAP2.2 and RAP2.12.

Figure S2. Multiple sequence alignment of the ERFVII-DNA binding domain and AlphaFold3 joint structure prediction for RAP2.12, AtMED25 and target DNA.

Figure S3. Semi-quantitative RT-PCR analysis of *AtMED25* transcript levels in the T-DNA insertion lines *med25-1* and *med25-2*.

Figure S4. Plot of RNA-Seq data for selected hypoxia core genes in hypoxia-treated *med25-1* and wildtype.

Figure S5. Position of primer pairs used in RNA Pol II ChIP assay.

Figure S6. Yeast two-hybrid assays for testing interaction between Mediator complex *At*MED25 with other Mediator subunits from Arabidopsis.

Figure S7. Identified potential interaction partners of *At*MED25 under normoxic and hypoxic conditions.

Figure S8. Multiple sequence alignment of MED25 proteins from different plant species.

Table S1. Oligonucleotide sequences used for cloning constructs in pENTR/D-TOPO and other vectors.

Table S2. Sequences of oligonucleotides used for RT-qPCR expression analysis of ethylene-induced genes.

Table S3. Sequences and positions of motifs and oligonucleotides used for ChIP-qPCR analysis.

REFERENCES

Abramson, J., Adler, J., Dunger, J., Evans, R., Green, T., Pritzel, A. *et al.* (2024) Accurate structure prediction of biomolecular interactions with AlphaFold 3. *Nature*, **630**, 493–500.

Agrawal, R., Jiří, F. & Thakur, J.K. (2021) The kinase module of the mediator complex: an important signalling processor for the development and survival of plants. *Journal of Experimental Botany*, **72**, 224–240.

Agrawal, R., Sharma, M., Dwivedi, N., Maji, S., Thakur, P., Junaid, A. *et al.* (2022) MEDIATOR SUBUNIT17 integrates jasmonate and auxin signaling pathways to regulate thermomorphogenesis. *Plant Physiology*, **189**, 2259–2280.

An, C., Li, L., Zhai, Q., You, Y., Deng, L., Wu, F. *et al.* (2017) Mediator subunit MED25 links the jasmonate receptor to transcriptionally active chromatin. *Proceedings of the National Academy of Sciences of the United States of America*, **114**, E8930–E8939.

Bäckström, S., Elfving, N., Nilsson, R., Wingsle, G. & Björklund, S. (2007) Purification of a plant mediator from *Arabidopsis thaliana* identifies PFT1 as the Med25 subunit. *Molecular Cell*, **26**, 717–729.

Baggerly, K.A., Deng, L., Morris, J.S. & Aldaz, C.M. (2003) Differential expression in SAGE: accounting for normal between-library variation. *Bioinformatics*, **19**(12), 1477–1483.

Bailey-Serres, J., Fukao, T., Gibbs, D.J., Holdsworth, M.J., Lee, S.C., Licausi, F. *et al.* (2012) Making sense of low oxygen sensing. *Trends in Plant Science*, **17**, 129–138.

Bailey-Serres, J., Fukao, T., Ronald, P., Ismail, A., Heuer, S. & Mackill, D. (2010) Submergence tolerant rice: SUB1's journey from landrace to modern cultivar. *Rice*, **3**, 138–147.

Barreto, P., **Dambire, C.**, **Sharma, G.**, **Vicente, J.**, **Osborne, R.**, **Yassitepe, J.** *et al.* (2022) Mitochondrial retrograde signaling through UCP1-mediated inhibition of the plant oxygen-sensing pathway. *Current Biology*, **32**, 1403–1411.

Blomberg, J., **Tasselius, V.**, **Vergara, A.**, **Karamat, F.**, **Imran, Q.M.**, **Strand, Å.** *et al.* (2023) *Pseudomonas syringae* infectivity correlates to altered transcript and metabolite levels of Arabidopsis mediator mutants. *bioRxiv.* Available from: https://doi.org/10.1101/2023.11.03.565469

Bui, L.T., **Giuntoli, B.**, **Kosmacz, M.**, **Parlanti, S.** & **Licausi, F.** (2015) Constitutively expressed ERF-VII transcription factors redundantly activate the core anaerobic response in *Arabidopsis thaliana*. *Plant Science*, **236**, 37–43.

Cerdan, P.D. & **Chory, J.** (2003) Regulation of flowering time by light quality. *Nature*, **423**, 881–885.

Çevik, V., **Kidd, B.N.**, **Zhang, P.**, **Hill, C.**, **Kiddle, S.**, **Denby, K.J.** *et al.* (2012) MEDIATOR25 acts as an integrative hub for the regulation of jasmonate-responsive gene expression in Arabidopsis. *Plant Physiology*, **160**, 541–555.

Chen, R., **Jiang, H.**, **Li, L.**, **Zhai, Q.**, **Qi, L.**, **Zhou, W.** *et al.* (2012) The Arabidopsis mediator subunit MED25 differentially regulates jasmonate and abscisic acid signaling through interacting with the MYC2 and ABI5 transcription factors. *Plant Cell*, **24**, 2898–2916.

Cho, H.Y., **Chou, M.Y.**, **Ho, H.Y.**, **Chen, W.C.** & **Shih, M.C.** (2022) Ethylene modulates translation dynamics in Arabidopsis under submergence via GCN2 and EIN2. *Science Advances*, **8**, eabm7863.

Deng, L., **Yang, T.**, **Li, Q.**, **Chang, Z.**, **Sun, C.**, **Jiang, H.** *et al.* (2023) Tomato MED25 regulates fruit ripening by interacting with EIN3-like transcription factors. *Plant Cell*, **35**, 1038–1057.

Dolan, W.L., **Dilkes, B.P.**, **Stout, J.M.**, **Bonawitz, N.D.** & **Chapple, C.** (2017) Mediator complex subunits MED2, MED5, MED16, and MED23 genetically interact in the regulation of phenylpropanoid biosynthesis. *Plant Cell*, **29**, 3269–3285.

Dotson, M.R., **Yuan, C.X.**, **Roeder, R.G.**, **Myers, L.C.**, **Gustafsson, C.M.**, **Jiang, Y.W.** *et al.* (2000) Structural organization of yeast and mammalian mediator complexes. *Proceedings of the National Academy of Sciences of the United States of America*, **97**, 14307–14310.

Elfving, N., **Davoine, C.**, **Benlloch, R.**, **Blomberg, J.**, **Brännström, K.**, **Müller, D.** *et al.* (2011) The *Arabidopsis thaliana* Med25 mediator subunit integrates environmental cues to control plant development. *Proceedings of the National Academy of Sciences of the United States of America*, **108**, 8245–8250.

Eysholdt-Derzsó, E., **Renziehausen, T.**, **Frings, S.**, **Frohn, S.**, **von Bongartz, K.**, **Igisch, C.P.** *et al.* (2023) Endoplasmic reticulum-bound ANAC013 factor is cleaved by RHOMBOID-LIKE 2 during the initial response to hypoxia in *Arabidopsis thaliana*. *Proceedings of the National Academy of Sciences of the United States of America*, **120**, e2221308120.

Fukao, T., **Yeung, E.** & **Bailey-Serres, J.** (2011) The submergence tolerance regulator SUB1A mediates crosstalk between submergence and drought tolerance in rice. *Plant Cell*, **23**, 412–427.

Galbraith, M.D., **Allen, M.A.**, **Bensard, C.L.**, **Wang, X.**, **Schwinn, M.K.**, **Qin, B.** *et al.* (2013) HIF1A employs CDK8-mediator to stimulate RNAPII elongation in response to hypoxia. *Cell*, **153**, 1327–1339.

Gasch, P., **Fundinger, M.**, **Müller, J.T.**, **Lee, T.**, **Bailey-Serres, J.** & **Mustroph, A.** (2016) Redundant ERF-VII transcription factors bind to an evolutionarily conserved cis-motif to regulate hypoxia-responsive gene expression in Arabidopsis. *Plant Cell*, **28**, 160–180.

Gibbs, D.J., **Lee, S.C.**, **Isa, N.M.**, **Gramuglia, S.**, **Fukao, T.**, **Bassel, G.W.** *et al.* (2011) Homeostatic response to hypoxia is regulated by the N-end rule pathway in plants. *Nature*, **479**, 415–418.

Gibbs, D.J., **Md Isa, N.**, **Movahedi, M.**, **Lozano-Juste, J.**, **Mendiondo, G.M.**, **Berckhan, S.** *et al.* (2014) Nitric oxide sensing in plants is mediated by proteolytic control of group VII ERF transcription factors. *Molecular Cell*, **53**, 369–379.

Giuntoli, B. & **Perata, P.** (2018) Group VII ethylene response factors in Arabidopsis: regulation and physiological roles. *Plant Physiology*, **176**, 1143–1155.

Gonzalez, D., **Bowen, A.J.**, **Carroll, T.S.** & **Conlan, R.S.** (2007) The transcription corepressor LEUNIG interacts with the histone deacetylase HDA19 and mediator components MED14 (SWP) and CDK8 (HEN3) to repress transcription. *Molecular and Cellular Biology*, **27**, 5306–5315.

Guo, J.X., **Song, R.F.**, **Lu, K.K.**, **Zhang, Y.**, **Chen, H.H.**, **Zuo, J.X.** *et al.* (2022) CycC;1 negatively modulates ABA signaling by interacting with and inhibiting ABI5 during seed germination. *Plant Physiology*, **190**, 2812–2827.

Harper, T.M. & **Taatjes, D.J.** (2018) The complex structure and function of mediator. *The Journal of Biological Chemistry*, **293**, 13778–13785.

Hartman, S., **Liu, Z.**, **van Veen, H.**, **Vicente, J.**, **Reinen, E.**, **Martopawiro, S.** *et al.* (2019) Ethylene-mediated nitric oxide depletion pre-adapts plants to hypoxia stress. *Nature Communications*, **10**, 4020.

He, H., **Denecker, J.**, **Van Der Kelen, K.**, **Willems, P.**, **Pottie, R.**, **Phua, S.Y.** *et al.* (2021) The Arabidopsis mediator complex subunit 8 regulates oxidative stress responses. *Plant Cell*, **33**, 2032–2057.

Hemsley, P.A., **Hurst, C.H.**, **Kaliyadasa, E.**, **Lamb, R.**, **Knight, M.R.**, **De Cothi, E.A.** *et al.* (2014) The Arabidopsis mediator complex subunits MED16, MED14, and MED2 regulate mediator and RNA polymerase II recruitment to CBF-responsive cold-regulated genes. *Plant Cell*, **26**, 465–484.

Henke, R.M., **Dastidar, R.G.**, **Shah, A.**, **Cadinu, D.**, **Yao, X.**, **Hooda, J.** *et al.* (2011) Hypoxia elicits broad and systematic changes in protein subcellular localization. *American Journal of Physiology. Cell Physiology*, **301**, C913–C928.

Hinz, M., **Wilson, I.W.**, **Yang, J.**, **Buerstenbinder, K.**, **Llewellyn, D.**, **Dennis, E.S.** *et al.* (2010) Arabidopsis RAP2.2: an ethylene response transcription factor that is important for hypoxia survival. *Plant Physiology*, **153**, 757–772.

Huang, S., **Zhu, S.**, **Kumar, P.** & **MacMicking, J.D.** (2021) A phase-separated nuclear GBPL circuit controls immunity in plants. *Nature*, **594**, 424–429.

Iñigo, S., **Giraldez, A.N.**, **Chory, J.** & **Cerdán, P.D.** (2012) Proteasome-mediated turnover of Arabidopsis MED25 is coupled to the activation of FLOWERING LOCUS T transcription. *Plant Physiology*, **160**, 1662–1673.

Ito, J., **Fukaki, H.**, **Onoda, M.**, **Li, L.**, **Li, C.**, **Tasaka, M.** *et al.* (2016) Auxin-dependent compositional change in mediator in ARF7- and ARF19-mediated transcription. *Proceedings of the National Academy of Sciences of the United States of America*, **113**, 6562–6567.

James, P., **Halladay, J.** & **Craig, E.A.** (1996) Genomic libraries and a host strain designed for highly efficient two-hybrid selection in yeast. *Genetics*, **144**, 1425–1436.

Karimi, M., **Inzé, D.** & **Depicker, A.** (2002) GATEWAY vectors for *Agrobacterium*-mediated plant transformation. *Trends in Plant Science*, **7**, 193–195.

Kaufmann, K., **Muiño, J.M.**, **Østerås, M.**, **Farinelli, L.**, **Krajewski, P.** & **Angenent, G.C.** (2010) Chromatin immunoprecipitation (ChIP) of plant transcription factors followed by sequencing (ChIP-SEQ) or hybridization to whole genome arrays (ChIP-CHIP). *Nature Protocols*, **5**, 457–472.

Kazan, K. (2017) The multitalented MEDIATOR25. *Frontiers in Plant Science*, **8**, 999.

Kidd, B.N., **Edgar, C.I.**, **Kumar, K.K.**, **Aitken, E.A.**, **Schenk, P.M.**, **Manners, J.M.** *et al.* (2009) The mediator complex subunit PFT1 is a key regulator of jasmonate-dependent defense in Arabidopsis. *Plant Cell*, **21**, 2237–2252.

Kim, M.J., **Jang, I.C.** & **Chua, N.H.** (2016) The mediator complex MED15 subunit mediates activation of downstream lipid-related genes by the WRINKLED1 transcription factor. *Plant Physiology*, **171**, 1951–1964.

Kim, N.Y., **Jang, Y.J.** & **Park, O.K.** (2018) AP2/ERF family transcription factors ORA59 and RAP2.3 interact in the nucleus and function together in ethylene responses. *Front. Plant Science*, **9**, 1675.

Kornberg, R.D. (2005) Mediator and the mechanism of transcriptional activation. *Trends in Biochemical Sciences*, **30**, 235–239.

Kosmacz, M., **Parlanti, S.**, **Schwarzländer, M.**, **Kragler, F.**, **Licausi, F.** & **Van Dongen, J.T.** (2015) The stability and nuclear localization of the transcription factor RAP2.12 are dynamically regulated by oxygen concentration. *Plant, Cell & Environment*, **38**, 1094–1103.

Lee, T.A. & **Bailey-Serres, J.** (2019) Integrative analysis from the epigenome to translatome uncovers patterns of dominant nuclear regulation during transient stress. *Plant Cell*, **31**, 2573–2595.

Leydon, A.R., **Wang, W.**, **Gala, H.P.**, **Gilmour, S.**, **Juarez-Solis, S.**, **Zahler, M.L.** *et al.* (2021) Repression by the Arabidopsis TOPLESS corepressor requires association with the core mediator complex. *eLife*, **10**, e66739.

Li, X., **Yang, R.** & **Chen, H.** (2018) The *Arabidopsis thaliana* Mediator subunit MED8 regulates plant immunity to *Botrytis cinerea* through interacting with the basic helix-loop-helix (bHLH) transcription factor FAMA. *PLoS One*, **13**, e0193458.

Licausi, F., **Kosmacz, M.**, **Weits, D.A.**, **Giuntoli, B.**, **Giorgi, F.M.**, **Voesenek, L.A.** *et al.* (2011) Oxygen sensing in plants is mediated by an N-end rule pathway for protein destabilization. *Nature*, **479**, 419–422.

Licausi, F., van Dongen, J.T., Giuntoli, B., Novi, G., Santaniello, A., Geigenberger, P. et al. (2010) HRE1 and HRE2, two hypoxia-inducible ethylene response factors, affect anaerobic responses in *Arabidopsis thaliana*. *The Plant Journal*, **62**, 302–315.

Lin, C.C., Chao, Y.T., Chen, W.C., Ho, H.Y., Chou, M.Y., Li, Y.R. et al. (2019) Regulatory cascade involving transcriptional and N-end rule pathways in rice under submergence. *Proceedings of the National Academy of Sciences of the United States of America*, **116**, 3300–3309.

Liu, B., Jiang, Y., Tang, H., Tong, S., Lou, S., Shao, C. et al. (2021) The ubiquitin E3 ligase SR1 modulates the submergence response by degrading phosphorylated WRKY33 in Arabidopsis. *Plant Cell*, **33**, 1771–1789.

Liu, K., Harrison, M.T., Yan, H., Liu, L., Meinke, H., Hoogenboom, G. et al. (2023) Silver lining to a climate crisis in multiple prospects for alleviating crop waterlogging under future climates. *Nature Communications*, **14**, 765.

Liu, Z., Hartman, S., van Veen, H., Zhang, H., Leeggangers, H.A.C.F., Martopawiro, S. et al. (2022) Ethylene augments root hypoxia tolerance via growth cessation and reactive oxygen species amelioration. *Plant Physiology*, **190**, 1365–1383.

Livak, K.J. & Schmittgen, T.D. (2001) Analysis of relative gene expression data using real-time quantitative PCR and the $2^{(-\Delta\Delta C(T))}$ method. *Methods*, **25**, 402–408.

Locke, A.M., Barding, G.A., Jr., Sathnur, S., Larive, C.K. & Bailey-Serres, J. (2018) Rice SUB1A constrains remodelling of the transcriptome and metabolome during submergence to facilitate post-submergence recovery. *Plant, Cell & Environment*, **41**, 721–736.

Loreti, E. & Perata, P. (2023) ERFVII transcription factors and their role in the adaptation to hypoxia in Arabidopsis and crops. *Frontiers in Genetics*, **14**, 1213839.

Marín-de la Rosa, N., Sotillo, B., Miskolczi, P., Gibbs, D.J., Vicente, J., Carbonero, P. et al. (2014) Large-scale identification of gibberellin-related transcription factors defines group VII ETHYLENE RESPONSE FACTORS as functional DELLA partners. *Plant Physiology*, **166**, 1022–1032.

Mathur, S., Vyas, S., Kapoor, S. & Tyagi, A.K. (2011) The mediator complex in plants: structure, phylogeny, and expression profiling of representative genes in a dicot (Arabidopsis) and a monocot (rice) during reproduction and abiotic stress. *Plant Physiology*, **157**, 1609–1627.

Miller, C., Matic, I., Maier, K.C., Schwalb, B., Roether, S., Strässer, K. et al. (2012) Mediator phosphorylation prevents stress response transcription during non-stress conditions. *The Journal of Biological Chemistry*, **287**, 44017–44026.

Mustroph, A., Zanetti, M.E., Jang, C.J., Holtan, H.E., Repetti, P.P., Galbraith, D.W. et al. (2009) Profiling translatomes of discrete cell populations resolves altered cellular priorities during hypoxia in Arabidopsis. *Proceedings of the National Academy of Sciences of the United States of America*, **106**, 18843–18848.

Nakano, T., Suzuki, K., Fujimura, T. & Shinshi, H. (2006) Genome-wide analysis of the ERF gene family in Arabidopsis and rice. *Plant Physiology*, **140**, 411–432.

Neuser, J., Metzen, C.C., Dreyer, B.H., Feulner, C., van Dongen, J.T., Schmidt, R.R. et al. (2019) HBI1 mediates the trade-off between growth and immunity through its impact on apoplastic ROS homeostasis. *Cell Reports*, **28**, 1670–1678.

Ou, B., Yin, K.Q., Liu, S.N., Yang, Y., Gu, T., Wing Hui, J.M. et al. (2011) A high-throughput screening system for Arabidopsis transcription factors and its application to Med25-dependent transcriptional regulation. *Molecular Plant*, **4**, 546–555.

Papdi, C., Pérez-Salamó, I., Joseph, M.P., Giuntoli, B., Bögre, L., Koncz, C. et al. (2015) The low oxygen, oxidative and osmotic stress responses synergistically act through the ethylene response factor VII genes RAP2.12, RAP2.2 and RAP2.3. *The Plant Journal*, **82**, 772–784.

Perez-Perri, J.I., Dengler, V.L., Audetat, K.A., Pandey, A., Bonner, E.A., Urh, M. et al. (2016) The TIP60 complex is a conserved coactivator of HIF1A. *Cell Reports*, **16**, 37–47.

Raya-Gonzalez, J., Ortiz-Castro, R., Ruiz-Herrera, L.F., Kazan, K. & Lopez-Bucio, J. (2014) PHYTOCHROME AND FLOWERING TIME1/MEDIATOR25 regulates lateral root formation via auxin signaling in Arabidopsis. *Plant Physiology*, **165**, 880–894.

Renziehausen, T., Frings, S. & Schmidt-Schippers, R. (2024) 'Against all floods': plant adaptation to flooding stress and combined abiotic stresses. *The Plant Journal*, **117**, 1836–1855. Available from: https://doi.org/10.1111/tpj.16614

Richter, W.F., Nayak, S., Iwasa, J. & Taatjes, D.J. (2022) The mediator complex as a master regulator of transcription by RNA polymerase II. *Nature Reviews. Molecular Cell Biology*, **23**, 732–749.

Saeed, A.I., Sharov, V., White, J., Li, J., Liang, W., Bhagabati, N. et al. (2017) TM4: a free, open-source system for microarray data management and analysis. *Biotechniques*, **34**, 374–378.

Sasidharan, R., Schippers, J.H.M. & Schmidt, R.R. (2021) Redox and low-oxygen stress: signal integration and interplay. *Plant Physiology*, **186**, 66–78.

Sato, S., Tomomori-Sato, C., Tsai, K.L., Yu, X., Sardiu, M., Saraf, A. et al. (2016) Role for the MED21-MED7 hinge in assembly of the mediator-RNA polymerase II holoenzyme. *The Journal of Biological Chemistry*, **291**, 26886–26898.

Schmidt, R., Mieulet, D., Hubberten, H.M., Obata, T., Hoefgen, R., Fernie, A.R. et al. (2013) SALT-RESPONSIVE ERF1 regulates reactive oxygen species-dependent signaling during the initial response to salt stress in rice. *Plant Cell*, **25**, 2115–2131.

Schmidt, R.R., Fulda, M., Paul, M.V., Anders, M., Plum, F., Weits, D.A. et al. (2018) Low-oxygen response is triggered by an ATP-dependent shift in oleoyl-CoA in Arabidopsis. *Proceedings of the National Academy of Sciences of the United States of America*, **115**, E12101–E12110.

Seguela-Arnaud, M., Smith, C., Uribe, M.C., May, S., Fischl, H., McKenzie, N. et al. (2015) The mediator complex subunits MED25/PFT1 and MED8 are required for transcriptional responses to changes in cell wall arabinose composition and glucose treatment in *Arabidopsis thaliana*. *BMC Plant Biology*, **15**, 215.

Shannon, P., Markiel, A., Ozier, O., Baliga, N.S., Wang, J.T., Ramage, D. et al. (2003) Cytoscape: a software environment for integrated models of biomolecular interaction networks. *Genome Research*, **13**, 2498–2504.

Soma, F., Takahashi, F., Suzuki, T., Shinozaki, K. & Yamaguchi-Shinozaki, K. (2020) Plant Raf-like kinases regulate the mRNA population upstream of ABA-unresponsive SnRK2 kinases under drought stress. *Nature Communications*, **11**, 1373.

Sundaravelpandian, K., Chandrika, N.N.P. & Schmidt, W. (2013) PFT1, a transcriptional mediator complex subunit, controls root hair differentiation through reactive oxygen species (ROS) distribution in Arabidopsis. *The New Phytologist*, **197**, 151–161.

Suzuki, G., Fukuda, M., Lucob-Agustin, N., Inukai, Y. & Gomi, K. (2022) The mutation of rice MEDIATOR25, OsMED25, induces Rice bacterial blight resistance through altering jasmonate- and auxin-signaling. *Plants (Basel)*, **11**, 1601.

Tang, H., Bi, H., Liu, B., Lou, S., Song, Y., Tong, S. et al. (2021) WRKY33 interacts with WRKY12 protein to up-regulate RAP2.2 during submergence induced hypoxia response in *Arabidopsis thaliana*. *The New Phytologist*, **229**, 106–125.

Tian, T., Liu, Y., Yan, H., You, Q., Yi X1 Du, Z., Xu, W. et al. (2017) agriGO v2.0: a GO analysis toolkit for the agricultural community, 2017 update. *Nucleic Acids Research*, **45**, W122–W129.

Vojnic, E., Mourão, A., Seizl, M., Simon, B., Wenzeck, L., Larivière, L. et al. (2011) Structure and VP16 binding of the mediator Med25 activator interaction domain. *Nature Structural & Molecular Biology*, **18**, 404–409.

Walter, M., Chaban, C., Schutze, K., Batistic, O., Weckermann, K., Nake, C. et al. (2004) Visualization of protein interactions in living plant cells using bimolecular fluorescence complementation. *The Plant Journal*, **40**, 428–438.

Wang, H., Li, S., Li, Y., Xu, Y., Wang, Y., Zhang, R. et al. (2019) MED25 connects enhancer-promoter looping and MYC2-dependent activation of jasmonate signalling. *Nature Plants*, **5**, 616–625.

Wang, T.Y., Wu, J.R., Duong, N.K.T., Lu, C.A., Yeh, C.H. & Wu, S.J. (2021) HSP70-4 and farnesylated AtJ3 constitute a specific HSP70/HSP40-based chaperone machinery essential for prolonged heat stress tolerance in Arabidopsis. *Journal of Plant Physiology*, **261**, 153430.

Weltmeier, F., Ehlert, A., Mayer, C.S., Dietrich, K., Wang, X., Schütze, K. et al. (2006) Combinatorial control of Arabidopsis proline dehydrogenase transcription by specific heterodimerisation of bZIP transcription factors. *The EMBO Journal*, **25**, 3133–3143.

Wendrich, J.R., Boeren, S., Möller, B.K., Weijers, D. & De Rybel, B. (2017) In vivo identification of plant protein complexes using IP-MS/MS. *Methods in Molecular Biology*, **1497**, 147–158.

White, M.D., **Kamps, J.J.A.G.**, **East, S.**, **Taylor Kearney, L.J.** & **Flashman, E.** (2018) The plant cysteine oxidases from *Arabidopsis thaliana* are kinetically tailored to act as oxygen sensors. *The Journal of Biological Chemistry*, **293**, 11786–11795.

White, M.D., **Klecker, M.**, **Hopkinson, R.J.**, **Weits, D.A.**, **Mueller, C.**, **Naumann, C.** *et al.* (2017) Plant cysteine oxidases are dioxygenases that directly enable arginyl transferase-catalysed arginylation of N-end rule targets. *Nature Communications*, **8**, 14690.

Wu, F.H., **Shen, S.C.**, **Lee, L.Y.**, **Lee, S.H.**, **Chan, M.T.** & **Lin, C.S.** (2009) Tape-Arabidopsis Sandwich – a simpler Arabidopsis protoplast isolation method. *Plant Methods*, **5**, 16.

Xu, K., **Xu, X.**, **Fukao, T.**, **Canlas, P.**, **Maghirang-Rodriguez, R.**, **Heuer, S.** *et al.* (2006) Sub1A is an ethylene-response-factor-like gene that confers submergence tolerance to rice. *Nature*, **442**, 705–708.

Xu, R. & **Li, Y.** (2011) Control of final organ size by mediator complex subunit 25 in *Arabidopsis thaliana*. *Development*, **138**, 4545–4554.

Yang, Y., **Ou, B.**, **Zhang, J.**, **Si, W.**, **Gu, H.**, **Qin, G.** *et al.* (2014) The Arabidopsis mediator subunit MED16 regulates iron homeostasis by associating with EIN3/EIL1 through subunit MED25. *The Plant Journal*, **77**, 838–851.

Yuan, C., **Hu, Y.**, **Liu, Q.**, **Xu, J.**, **Zhou, W.**, **Yu, H.** *et al.* (2023) MED8 regulates floral transition in Arabidopsis by interacting with FPA. *The Plant Journal*, **116**, 1234–1247.

Zhai, Q., **Deng, L.** & **Li, C.** (2020) Mediator subunit MED25: at the nexus of jasmonate signaling. *Current Opinion in Plant Biology*, **57**, 78–86.

Zhang, P., **Ma, X.**, **Liu, L.**, **Mao, C.**, **Hu, Y.**, **Yan, B.** *et al.* (2023) MEDIATOR SUBUNIT 16 negatively regulates rice immunity by modulating PATHOGENESIS RELATED 3 activity. *Plant Physiology*, **192**, 1132–1150.

Zhang, X., **Zhou, W.**, **Chen, Q.**, **Fang, M.**, **Zheng, S.**, **Scheres, B.** *et al.* (2018) Mediator subunit MED31 is required for radial patterning of Arabidopsis roots. *Proceedings of the National Academy of Sciences of the United States of America*, **115**, E5624–E5633.

Zhang, Y., **Wu, H.**, **Wang, N.**, **Fan, H.**, **Chen, C.**, **Cui, Y.** *et al.* (2014) Mediator subunit 16 functions in the regulation of iron uptake gene expression in Arabidopsis. *The New Phytologist*, **203**, 770–783.

Zhong, S., **Lin, Z.**, **Fray, R.G.** & **Grierson, D.** (2008) Improved plant transformation vectors for fluorescent protein tagging. *Transgenic Research*, **17**, 985–989.

Zhou, Y., **Tan, W.J.**, **Xie, L.J.**, **Qi, H.**, **Yang, Y.C.**, **Huang, L.P.** *et al.* (2020) Polyunsaturated linolenoyl-CoA modulates ERF-VII-mediated hypoxia signaling in Arabidopsis. *Journal of Integrative Plant Biology*, **62**, 330–348.

Zhu, Y., **Schluttenhoffer, C.M.**, **Wang, P.**, **Fu, F.**, **Thimmapuram, J.**, **Zhu, J.K.** *et al.* (2014) CYCLIN-DEPENDENT KINASE8 differentially regulates plant immunity to fungal pathogens through KINASE-dependent and -independent functions in Arabidopsis. *Plant Cell*, **26**, 4149–4170.

Zubrycka, A., **Dambire, C.**, **Dalle Carbonare, L.**, **Sharma, G.**, **Boeckx, T.**, **Swarup, K.** *et al.* (2023) ERFVII action and modulation through oxygen-sensing in *Arabidopsis thaliana*. *Nature Communications*, **14**, 4665.